United States
Environmental Protection
Agency

Industrial Environmental Research
Laboratory
Research Triangle Park NC 27711

EPA-600/7-79-027
January 1979

EPA

Sampling Charged Particles with Cascade Impactors

Interagency Energy/Environment R&D Program Report

RESEARCH REPORTING SERIES

Research reports of the Office of Research and Development, U.S. Environmental Protection Agency, have been grouped into nine series. These nine broad categories were established to facilitate further development and application of environmental technology. Elimination of traditional grouping was consciously planned to foster technology transfer and a maximum interface in related fields. The nine series are:

1. Environmental Health Effects Research
2. Environmental Protection Technology
3. Ecological Research
4. Environmental Monitoring
5. Socioeconomic Environmental Studies
6. Scientific and Technical Assessment Reports (STAR)
7. Interagency Energy-Environment Research and Development
8. "Special" Reports
9. Miscellaneous Reports

This report has been assigned to the INTERAGENCY ENERGY-ENVIRONMENT RESEARCH AND DEVELOPMENT series. Reports in this series result from the effort funded under the 17-agency Federal Energy/Environment Research and Development Program. These studies relate to EPA's mission to protect the public health and welfare from adverse effects of pollutants associated with energy systems. The goal of the Program is to assure the rapid development of domestic energy supplies in an environmentally-compatible manner by providing the necessary environmental data and control technology. Investigations include analyses of the transport of energy-related pollutants and their health and ecological effects; assessments of, and development of, control technologies for energy systems; and integrated assessments of a wide range of energy-related environmental issues.

EPA REVIEW NOTICE

This report has been reviewed by the participating Federal Agencies, and approved for publication. Approval does not signify that the contents necessarily reflect the views and policies of the Government, nor does mention of trade names or commercial products constitute endorsement or recommendation for use.

This document is available to the public through the National Technical Information Service, Springfield, Virginia 22161.

EPA-600/7-79-027

January 1979

Sampling Charged Particles with Cascade Impactors

by

W.E. Farthing, D.H. Hussey, W.B. Smith,
and R.R. Wilson, Jr.

Southern Research Institute
2000 Ninth Avenue, South
Birmingham, Alabama 35205

Contract No. 68-02-2131
T.D. 10401 and 11301
Program Element No. EHE624

EPA Project Officer: D. Bruce Harris

Industrial Environmental Research Laboratory
Office of Energy, Minerals, and Industry
Research Triangle Park, NC 27711

Prepared for

U.S. ENVIRONMENTAL PROTECTION AGENCY
Office of Research and Development
Washington, DC 20460

TABLE OF CONTENTS

FIGURES

TABLES

ABSTRACT

In performing particle size distribution measurements at control devices operating on industrial process streams, investigators are usually aware that in some cases charged particles will be present in the gas stream. In order to assess the influence of particle charge, three different experiments were performed to determine whether or not cascade impactors sampling charged aerosols can yield erroneous particle size distribution measurements. The commercially available cascade impactors utilized in this study were the Andersen Mark III Stack Sampler, the Meteorology Research, Inc. Model 1502 Cascade Impactor, and the University of Washington Mark III Source Test Cascade Impactor. In general, the measured distributions indicated more large particles and fewer small particles than actually existed. The deviations from the true size distribution was found to be a function of the magnitude of charge. This deviation was smaller if glass fiber substrates were used as impactor collection surfaces instead of the metal collection plates alone. For charge levels representative of electrostatic precipitators operating at normal charging conditions (an electric field strength of 400,000 V/m and a current density of 3×10^{-4} A/m^2), the differences between the true and measured polydisperse size distributions with glass fiber substrates were small.

ACKNOWLEDGEMENT

Mr. Don Johnson helped to take much of the data. We are also grateful for the suggestions and advice of the project officer, Mr. D. Bruce Harris.

SECTION 1.

INTRODUCTION

This report contains a summary of research conducted on the collection of charged particles in cascade impactors. The scope of this report does not include an examination of the theories which would describe a charged particle's behavior as it travelled through and was finally collected in a cascade impactor. However, these experiments do indicate the relative deviation from the true size distribution one might expect to find in cascade impactor measurements of charged particles, especially those measurements made at the outlet of an industrial electrostatic precipitator.

Three sets of experiments were performed: one using monodisperse aerosols sampled by University of Washington Mark III, Andersen Mark III, and the MRI Model 1502 cascade impactors; a second involving sampling polydisperse aerosols with a Brink cascade impactor; and a third involving the sampling of polydisperse aerosols with Andersen Mark III cascade impactors. Section 2 contains a brief description of the experimental procedure and results, and Section 3 contains a number of conclusions that can be drawn from the data.

SECTION 2.
PROCEDURES AND RESULTS

MONODISPERSE AEROSOL

Experimental Procedure

Figure 1 shows the aerosol generating, charging, and sampling system. A monodisperse aerosol was generated with a Vibrating Orifice Aerosol Generator (VOAG). Ammonium fluorescein droplets were charged, dried, and then sampled with a cascade impactor. The collection efficiencies of the various impactor surfaces were then found by washing each surface individually with an ammonium hydroxide solution and measuring the optical absorbance of the wash to find the total mass on each surface. This procedure is similar to that described by Cushing, et al.[1]

Two particle sizes were used in the experiments, 5.2 and 2.1 μm. The 5.2 μm particles were charged to two different levels of charge, 40,000 and 7,000 electronic charges.* The 2.1 μm particles were charged and sampled at two charge levels also: 2,600 and 600 electronic charges. In each instance, the lower charge values were representative of those to be expected at precipitator outlets. The higher charge level was chosen in order

---

* For large particles (>2 μm in dia.) and common ESP operating conditions, the upper limit of charge is that of saturation in field charging. For a typical field strength (4×10^3 volts/cm), the number of charges per particle, n_p, is given by

$$n_p = 834\ r_p^2 \qquad (1)$$

where r_p is the particle radius in micrometers. This means that for particles with a 5 μm diameter n_p is approximately 5600 and for particles with a 2 μm diameter n_p is approximately 900. For smaller particles the particle charge is somewhat larger than Equation (1) predicts.

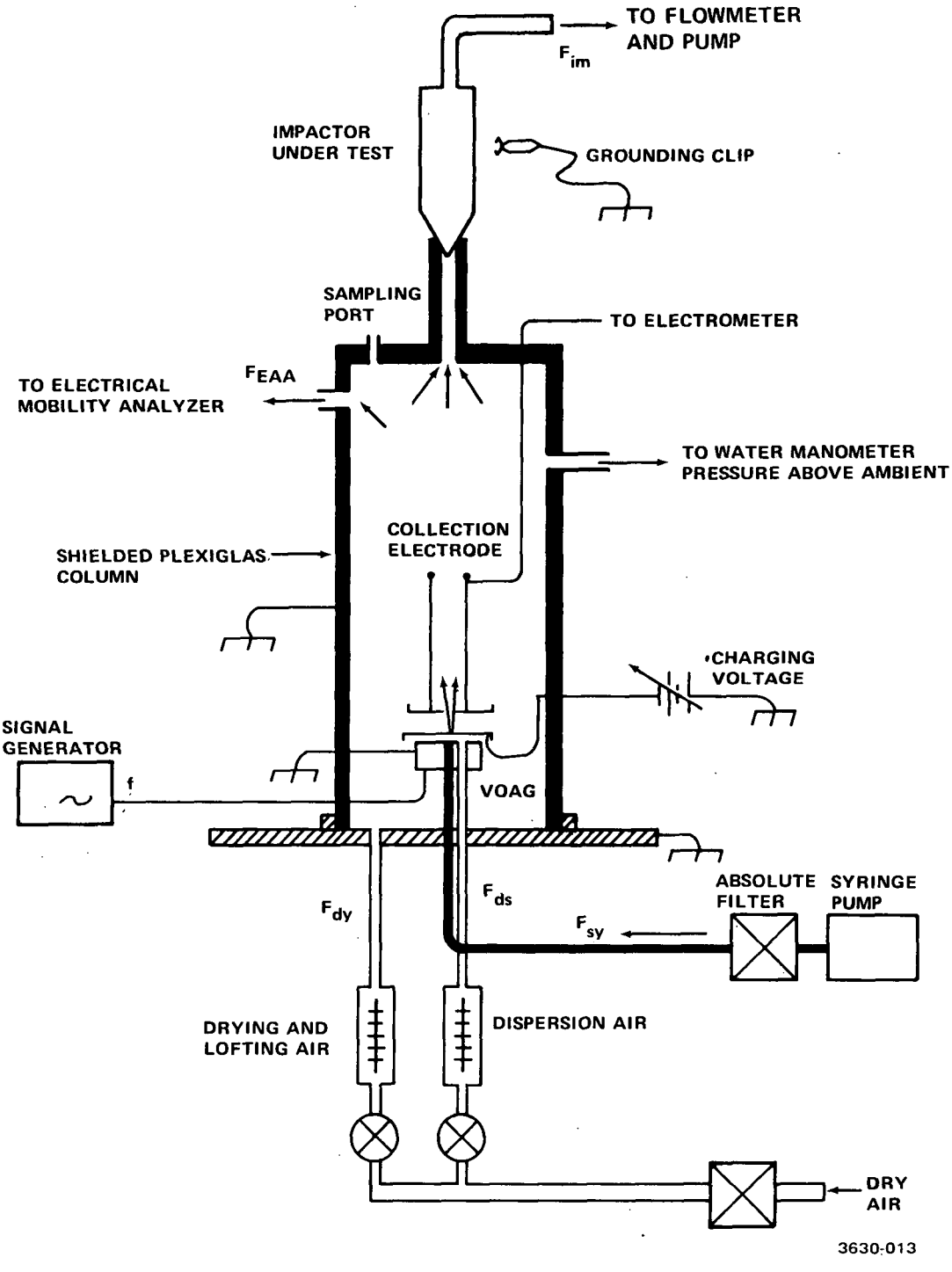

Figure 1. Schematic of the charged particle generator and sampling arrangement.

to investigate the potential for more serious effects if higher than usual charge levels should be encountered.

The operational procedure in the experiments was to sample the charged aerosol with and without a charge neutralizer near the impactor nozzle. In each test the entire impactor was used, and the impactors were operated at 0.5 cfm, the recommended flow rate. Tests were conducted with and without a grounding wire on the impactor.

The impactors investigated in this study were:

1. Andersen Mark III Stack Sampler (Andersen)
   Andersen 2000, Inc.
   Atlanta, GA 30320

2. MRI Model 1502 Inertial Cascade Impactor (MRI)
   Meteorology Research, Inc.
   Altadena, CA 91001

3. University of Washington Mark III Source Test
   Cascade Impactor
   (U. of W.)
   Pollution Control Systems, Inc.
   Renton, Washington 98055

In this discussion, the method of charging particles and measuring the charge is described first, then impactor data and conclusions are presented.

Particle Charging

The induction method of charging droplets produced with a VOAG was introduced by Reischl, et al.[2] The region of droplet formation of a VOAG is depicted in Figure 2, with the entire aerosol system shown in Figure 1. Ammonium fluorescein solution is pumped through an orifice mounted on a piezoelectric ceramic. Due to the applied sine wave voltage of frequency f, the

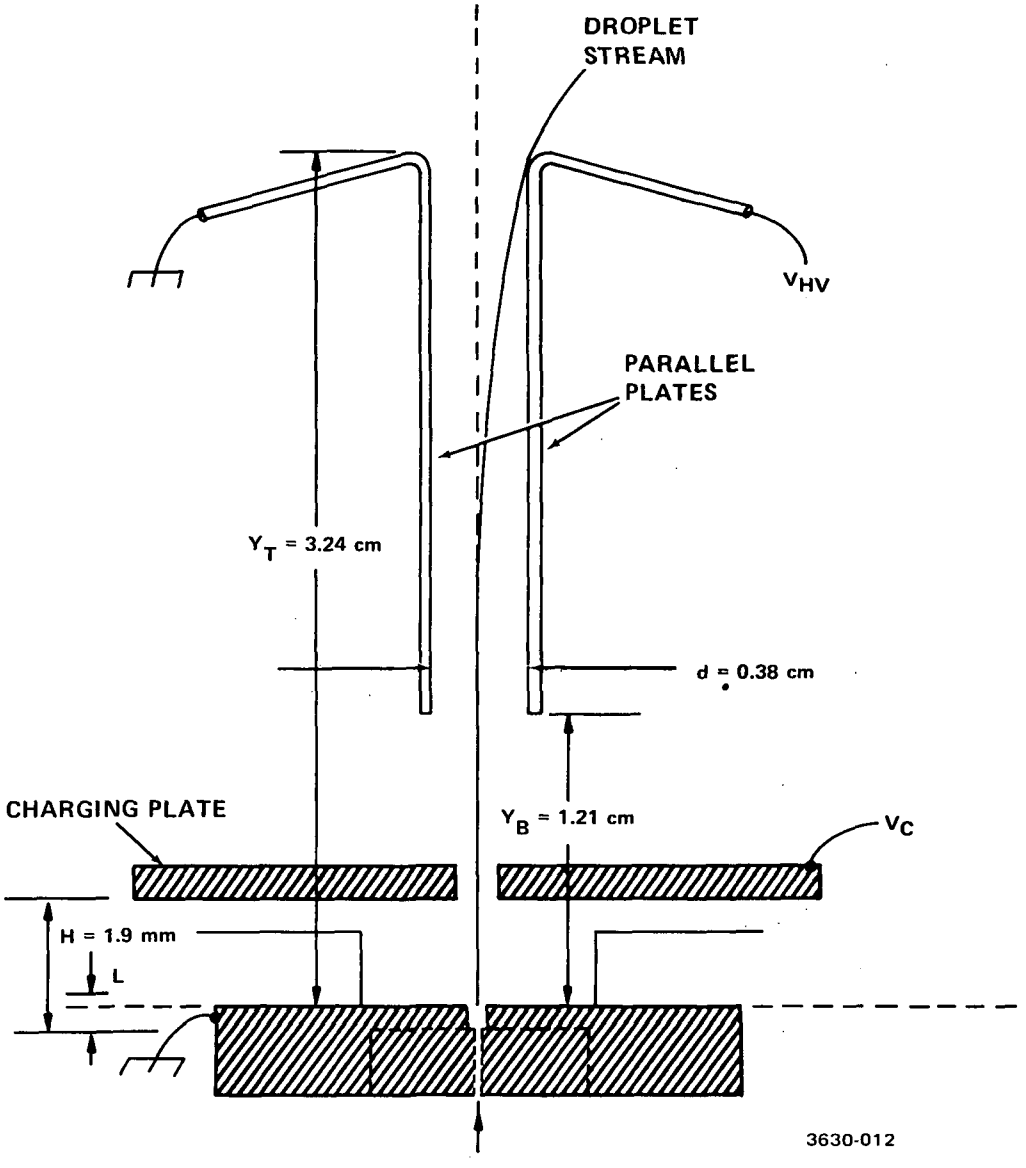

Figure 2. Charged particle generator orifice region with the parallel plates for charge measurement.

crystal oscillates, producing periodic perturbations of the liquid jet formed at the orifice. This causes the jet to become detached and form droplets at regular intervals. Droplet formation occurs at a height L above the orifice. The solvent, ammonium hydroxide, evaporates and leaves spherical particles of the solute, ammonium fluorescein. The particle radius r_p is then given by

$$\left(\frac{3C'F_{sy}}{4\pi f}\right)^{1/3} \qquad (2)$$

where F_{sy} is the liquid flowrate in ml per second and C' is the solute concentration. In this study f was always set at 65 kHz and F_{sy} at 0.201 ml per minute.

If the liquid is electrically conducting, then charge can be induced upon the droplet during its formation by applying an electric field. The expression for the induced charge per droplet, n_p, given by Reischl, et al[2] for a highly conducting liquid is

$$n_p = n_{p_o} - \frac{4\pi\epsilon_0 r_d}{e} \frac{L\alpha}{H} V_c \qquad (3)$$

where r_d = droplet radius = $\left(\frac{3F_{sy}}{4\pi f}\right)^{1/3}$,

H = height of top electrode plate above the orifice,

V_c = applied voltage,

e = elementary unit of charge, 1.602×10^{-19} coulombs,

ϵ_0 = dielectric constant of free space, 8.85×10^{-12} coulomb /Newton m^2

α = constant determined from the geometry of the orifice region = 0.81 for the device shown,

n_{p_o} = charge on particle from spraying process, and

$4\pi\epsilon_0 r_d$ = capacitance of a sphere.

Equation (3) is based on the model of the spherical droplet immersed in the electric field with a conducting lead (liquid jet) connected to it. This expression has not been verified on an absolute basis; however, the linear dependence of n_p upon V_c was substantiated by Reischl, et al.[2] Thus the measurement of charge

was necessary to calibrate the instrument for this study although r_d, L, H, α, and V_c were measured independently. Comparisons of the predictions of Equation (3) and the charge measurements are given in this report. The most difficult parameter to measure is L. A microscope (125X) allowed visual observation of the jet disturbance at the point of droplet formation and a rough measurement of L. However, this measurement cannot be made accurately without a strobe and camera arrangement, which was unavailable.

Reischl, et al,[2] measured the charge on dry particles; no measurements were made of the droplet charge. During a single run no variation in charge per particle was measured by them, indicating a variation of less than ±2%. From one run to another, however, a variation in n_{p_o} and the coefficient of V_c was observed (see Table I).

Charge Measurement Methods

In this study four different methods were developed to measure the charge per particle in order to provide independent checks as well as to establish a convenient procedure. Initially two methods were devised to measure charge on the dry particles of ammonium fluorescein: (I) sampling with a modified, commercial, electrical mobility analyzer[3] (EAA) and (II) absolute filtering of dried particles on an electrometer electrode. Difficulties were encountered with the EAA due to wall losses and inability to sample high concentrations of dry particles. Method II was time consuming. Because of these difficulties in charge measurement of dry particles, two new methods were then developed and applied which gave information about droplet charge: (III) deflection in a uniform field with a parallel plate mobility analyzer, and (IV) collection of undried aerosol droplets on an electrometer electrode. Previously, Zung and Snead[4] observed that the droplet charge was altered while drying. In this study a set of measurements were performed using Methods II and IV to evaluate that possibility. These methods are described below, and results and evaluations are given in the next section. Method

Table I. Average Values and Standard Deviations of Charging Parameters Observed by Reischl, *et al.*[2]

Solute	Number of runs	n_{p_o}	Coefficient of V_c in Eq. (2)
Methylene Blue	12	-1640 ± 360	-1830 ± 670
Potassium Biphthalate	11	-5540 ± 910	-2900 ± 770
Sodium Chloride	5	-2640 ± 160	-1140 ± 190

IV turned out to be the most suitable one for this project, while the others provided verification and had desirable possibilities for any future work performed in this area.

Method I

Method I employed a Thermo-Systems Model 3030 electrical aerosol analyzer (EAA) (See Figure 3). This particular device was designed to sample particles with diameters less than one micron. Several modifications were made to eliminate wall losses so that the electrical mobility of larger particles could be measured. With this device n_p is given by

$$n_p = z_p 6\pi\eta r_p / e C \qquad (4)$$

where C is the slip correction factor,

r_p is the particle radius known from the VOAG operating conditions,

η is the viscosity of air, and

z_p is the electrical mobility in m/volt-sec. The mobility is determined by

$$z_p = K/V = 3.98 \times 10^{-4}/V$$

where K is a constant depending upon the flow and geometry of the analyzer, and

V is the applied voltage in the analyzer at which all particles are collected; i.e., removed from the air flow so that the analyzer current goes to zero.

Method II

The charge on dry particles versus charging voltage was measured with a filter-electrode substituted for the impactor shown in Figure 1. This method employed a filter membrane made of silver and electrically connected to an electrometer. The ammonium fluorescein aerosol was sampled with the filter at the same flow rate as an impactor. An electrometer measured the total

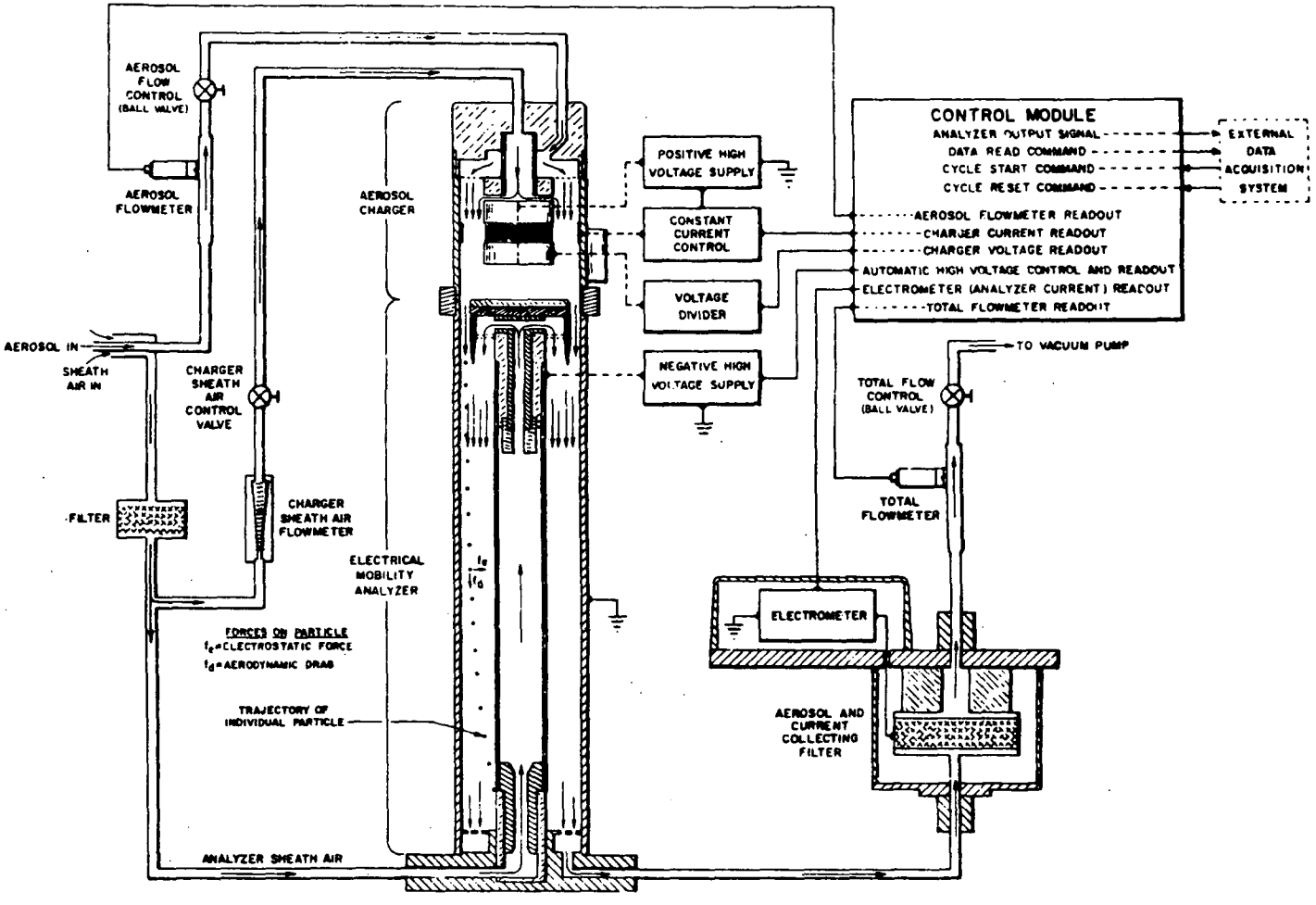

Figure 3. Flow schematic and electronic block diagram of the Electrical Aerosol Analyzer. From Sem[3].

charge collected by the filter. After sampling, the total mass of ammonium fluorescein collected was determined by washing the filter with an ammonium hydroxide solution and spectrophotometry of the wash solution. In this method n_p is given by

$$n_p = \frac{4\pi}{3} \frac{Q\rho_{AF}}{eM_t} r_p^3 \qquad (5)$$

where Q = charge collected,
ρ_{AF} = density of ammonium fluorescein,
r_p = particle radius, and
M_t = total mass collected.

Method III

The droplet stream passed between parallel plates as depicted in Figure 2. With a high voltage V_{HV} applied between the plates, the charged droplets could be deflected as indicated. The equations of motion for the droplets are:

$$U_y = \left(\frac{mg}{b} + U_{y_o}\right) e^{-bt/m} - \frac{mg}{b} \qquad (6)$$

$$y = \left(\frac{m^2 g}{b^2} + \frac{mU_{y_o}}{b}\right) \left(1 - e^{-bt/m}\right) - \frac{mg}{b}t \qquad (7)$$

$$U_x = \frac{n_p e V_{HV}}{bd} \left(1 - e^{-b(t-t_B)/m}\right) \qquad (8)$$

$$x = \frac{n_p e V_{HV}}{bd} \left[t - t_B - \frac{m}{b}\left(1 - e^{-b(t-t_B)/m}\right)\right] \qquad (9)$$

where U_x and U_y are the horizontal and vertical components of the droplet velocity,

t = time of flight, t_B = elapsed time when droplet is at the bottom of the plates,
U_{y_o} = initial droplet velocity = F_{sy}/π(orifice radius)^2,
m = droplet mass = (density of liquid) x (F_{sy}/f),
g = acceleration due to gravity,

b = $6\pi r_d \eta$, where η is the viscosity of air and r_d is the droplet diameter, and

d = separation between the plates.

With V_{HV} = 0 (no deflection) and U_{y_o} = 793 m/sec, it was found that the droplets rise much higher (y = 15 cm) than the equations predict (y = 5 cm) using the viscosity of air (182.7 x 10^{-6} poise) at standard pressure and temperature. The droplets rose higher because of the flow of drying and dispersion air in the same direction as the droplet stream. Therefore, the droplets experienced a lower viscous drag than they would in still air. An effective viscosity of 57 x 10^{-6} poise was determined which gives the correct height of the flight with V_{HV} = 0. Using the values of Y_T and Y_B (the height of the top and bottom of the plates, respectively), $t_T - t_B$ (where t_T is the elapsed time when the droplet is at the top of the plates) can be found from Equation 7. Then, with V_{HV} and d known, n_p can be calculated from Equation 9. Since the stream of charged droplets does not spread due to the applied field V_{HV}, the charge per droplet was uniform.

Method IV

Another method employed to measure droplet charge collected the droplets onto an aluminum foil electrometer electrode as they passed through the charging plate. The electrode was a hollow cylinder into which the particles entered through the bottom (see Figure 1). The top of the cylinder was covered with fine mesh metal netting (pore size, 0.16 mm, and 36% open) to allow air to flow through. With this arrangement n_p is given by

$$n_p = \frac{I}{fe} \qquad (10)$$

where I = electrometer current,

f = frequency of the oscillator driving the VOAG, and

e = elementary unit of charge.

The electrode was inserted and charge measured before and after an impactor sampling run.

Two variations of this method were attempted in search of a measurement method which can be used during impactor runs. An electrode with the same cylindrical shape was formed entirely of fine mesh metal netting. In one variation, a high voltage wire was placed along the cylinder axis. This wire, having the same polarity as the droplets, enhanced the collection efficiency of the netting. With the high voltage wire at zero volts a large portion of the charged aerosol passed through the net electrode and was sampled by the impactor. Then, to intermittently measure the droplet charge, the voltage on the wire was increased to collect the aerosol on the electrode. In the other variation of this method, the cylinder, made of metal netting, was used without the high voltage wire. The dispersion and drying air flowrate was lowered to give a high droplet collection efficiency for the electrode during charge measurement and then was changed to values which reduced the droplet collection of the electrode so that impactor sampling could proceed. Although both of these variations showed promise, time did not permit sufficient refinement to justify their use in the final analysis of impactor behavior.

Evaluation of the Charged Particle Generator

The behavior of the charged particle generator was characterized with the four methods of charge measurement described above. The results are depicted in Figures 4 and 5 where n_p is plotted as a function of charging voltage V_c. Figure 4 shows the full range of V_c employed, while Figure 5 gives a better view for small n_p.

The open triangle in Figure 4 depicts the charge measured on droplets using Method III. The single point given was determined from the average of three V_c-values taken on different

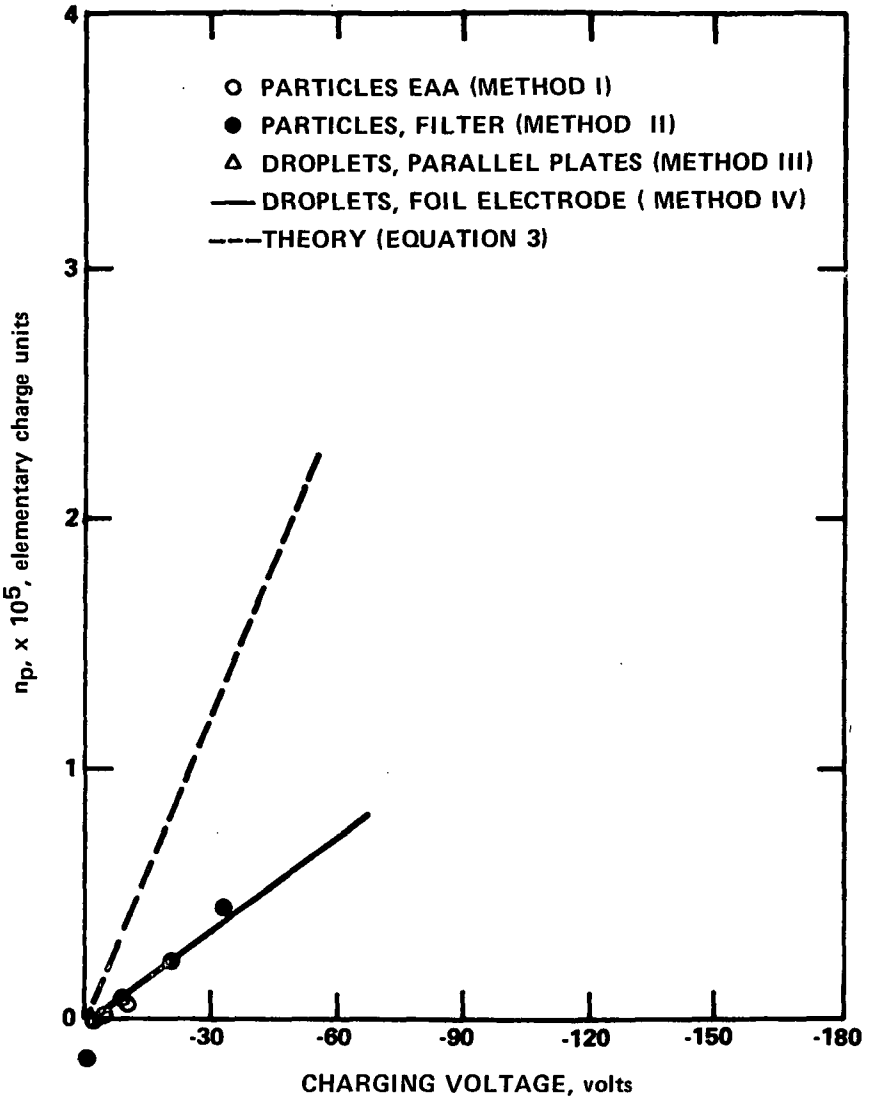

Figure 4. Particle charge versus charging voltage for the VOAG charged particle generator as determined by Methods I-IV (r_p = 2.6 μm and r_d = 23 μm).

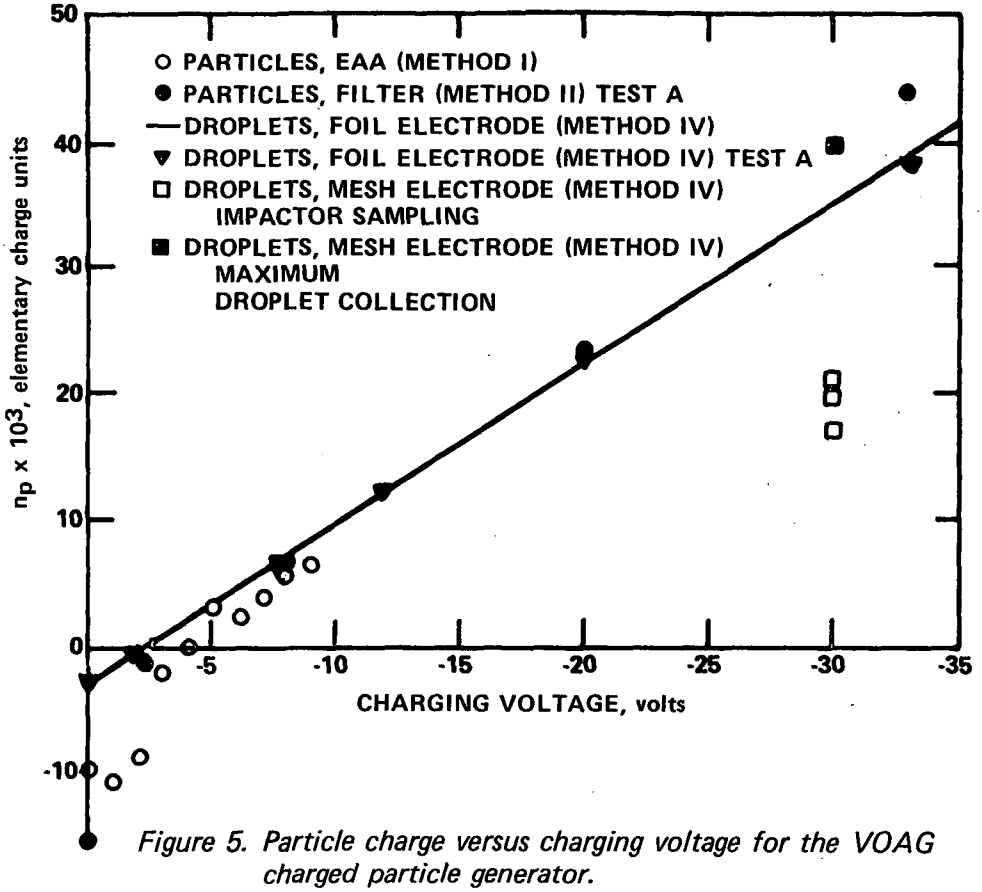

Figure 5. Particle charge versus charging voltage for the VOAG charged particle generator.

occasions with V_{HV} = 2000V. The procedure in this measurement was to adjust the charging voltage V_c to deflect the stream to the top of one plate as shown in Figure 2. This value varied from run to run by ±6%. The most likely source of error in this calculation is the estimation of the effective viscosity in Equation (6).

The measurements using Method IV (cylindrical electrode made of foil) are depicted by the solid line in Figures 4 and 5. This line is a least squares fit to Equation (3) from 33 measurements obtained in four different runs over a period of two weeks. The fluctuation of measured n_p values from this line were low as judged from the coefficient of determination (0.997 where 1.000 is a perfect fit). The value of n_{po} is -3050 ±580 and the coefficient of V_c (slope of the line) is 1280 ±20 volt^{-1}. These results are comparable to those of Reischl, et al[2] for sodium chloride (see Table I).

The measurements on dry particles, denoted by open circles, were obtained with the modified EAA (Method I). These results are more easily viewed in Figure 5 where the lower quarter of Figure 4 is reproduced. These measurements with the EAA are consistent with the results of the other methods. Although the preliminary results shown in Figure 4 and 5 were obtained by this method, attempts to repeat this measurement were unsuccessful. The problem was that no stable current of any significance (>10^{-14} amps) was produced by charged particles passing through the device. Apparently, the wall losses were too great and the number of particles sampled too small.

The data obtained by Method II for dry particles is depicted by closed circles in Figure 4. Although time consuming, these measurements were important because Zung and Snead[4] observed a change in the charge on the droplets while drying. The agreement between measurements using Methods II and IV eliminated this possibility for our experiments and thus justified the use of Method IV which determines particle charge from the droplet charge measurement.

The dashed line in Figure 4 gives the predictions of Equation (3) where the parameters L, H, and α were measured independently of n_p. Since n_{po}, the charge given to particles in the spraying process, cannot be predicted, its value in Figure 4 was estimated by extrapolating the Method IV foil electrode data to $V_c = 0$. The charge values for $V_c = 0$ were too low to be measured accurately. The difficulty in locating the end of the jet without high speed photography caused additional uncertainty in the measurements.

The data depicted by squares in Figure 5 are presented to illustrate data which may be obtained with the two described variations of Method IV. The data represented by open squares were measured using the metal-mesh electrode with a high voltage wire along the electrode axis. The three values given for n_p at constant V_c are for different values of this wire voltage: 0, 1000, and 2000 volts. The higher n_p values correspond to greater collection efficiencies, none of which are 100%. Total collection was obtained by adjusting the dispersion and drying air flowrates to maximize the electrometer current with the high voltage wire at zero volts. This single measurement is represented by the solid square. This data, concerning the variations of Method IV, is given only to illustrate the possibility for its use in further work if the ability to monitor particle charge is important.

The solid line representing Method IV data in Figure 5 was used as the calibration curve for the charged particle generator. Its agreement with Method II and the results of Reischl, et al[2] justified its use. In addition to the calibration, further measurements of particle charge with Method IV were performed before and after most impactor sampling runs.

Impactor Data

Impactor sampling data are given in Figures 6 through 20 in the form of histograms. Each figure shows data from one sampling test; the fraction of total particles collected is given for each surface in the impactor starting with the nozzle and ending with the housing of the absolute filter at the exit. The surfaces are distinguished according to nozzle, jet plate, substrate, and housing if separable. Each of these surfaces was washed separately and the mass of fluorescein in the wash water determined with a spectrophotometer.

The parameters varied in these tests were particle size (5.2 μm and 2.1 μm), particle charge, electrical grounding, and the use of a charge neutralizer. The sampling times, varied between one to one-and-a-half hours. However, the total number of particles sampled was smaller for highly charged particles, a result of greater wall losses in the drying chamber.

All sampling tests were performed at ambient conditions at a flow rate of 14 ℓ/min. The impactor nozzles were 1.27 cm (0.5 in.) in diameter giving a gas velocity of 1.84 m/sec. The stream velocity where sampling occurred was approximately one m/sec. Glass fiber substrates were employed in each test.

MRI Impactor

Figures 6 through 13 show MRI Model 1502 Cascade Impactor data (Figures 6-11 for 5.2 μm diameter and 12-13 for 2.1 μm diameter particles).

Figure 6 shows data for a "reference" run with no particle charge. The data shown in Figure 7 is for particles with about 4×10^4 charges and electrically isolated impactor. The increase in the number of particles collected on the nozzle and metal jet plates is quite significant. Also there was a slight increase in the number of particles reaching the stages below number three.

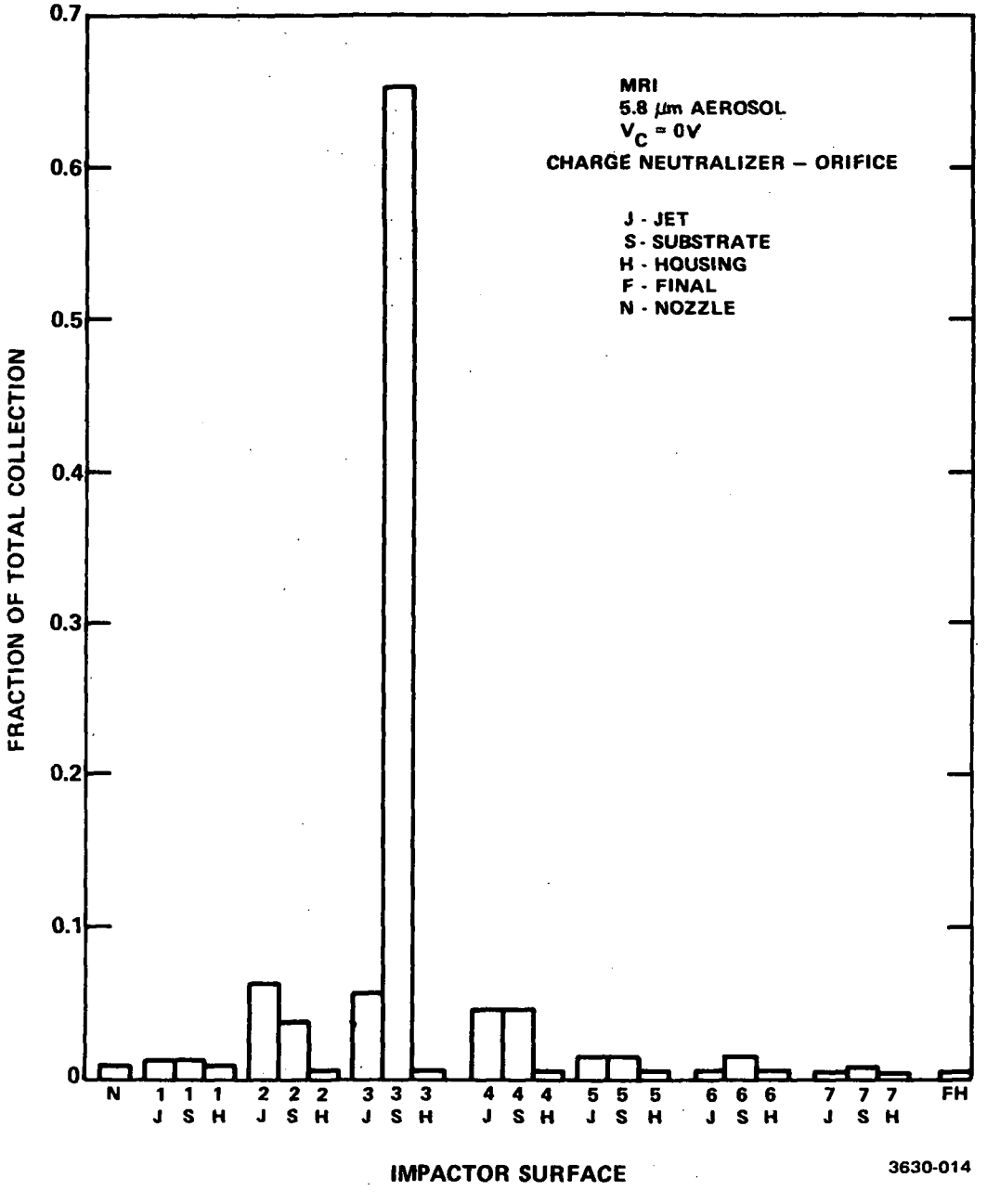

Figure 6. Control sampling run using MRI-Model 1502 Impactor with no charge.

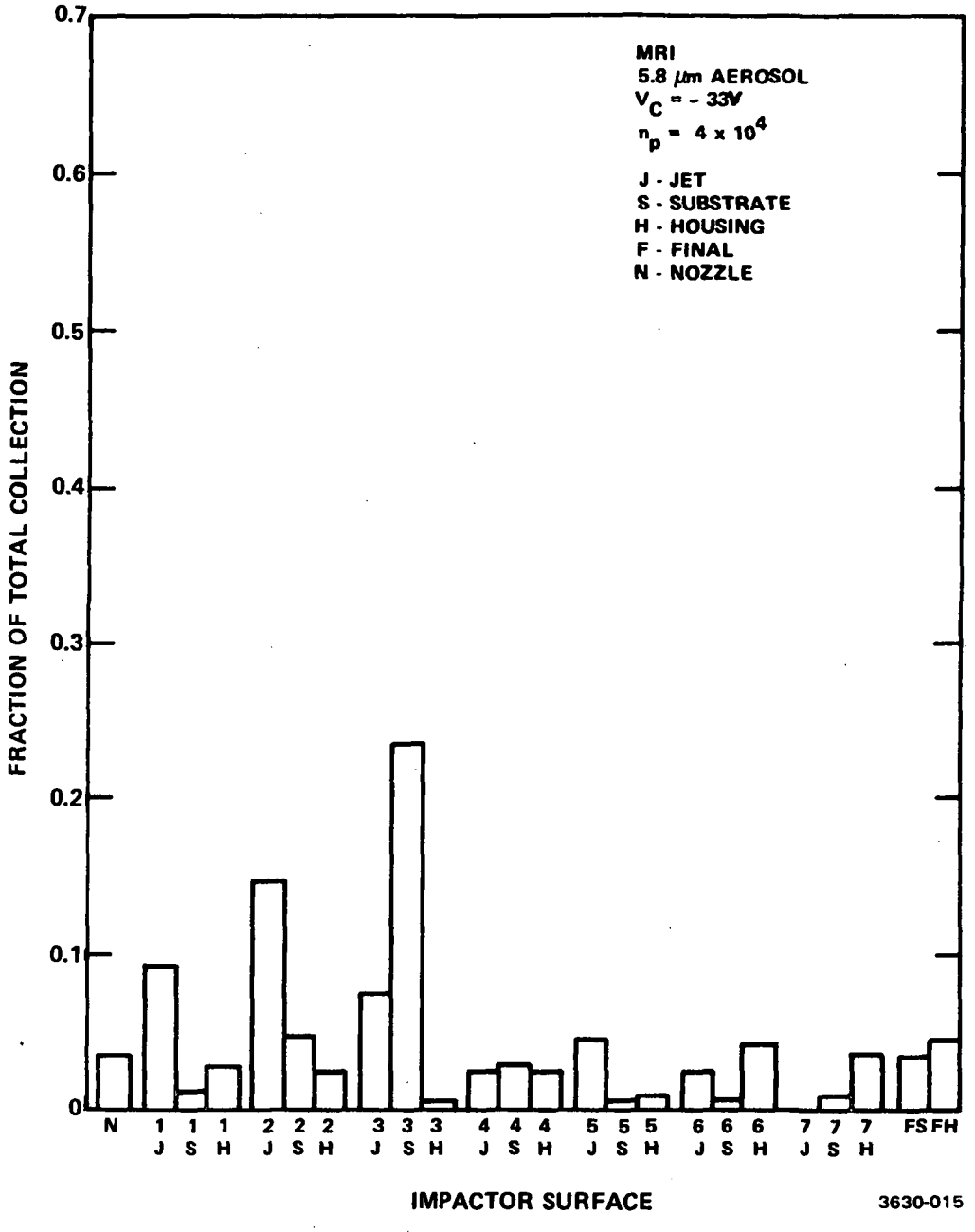

Figure 7. Sampling charged particles using MRI-Model 1502 Impactor with no grounding wire —— high particle charge. (See Figure 6 for comparison.)

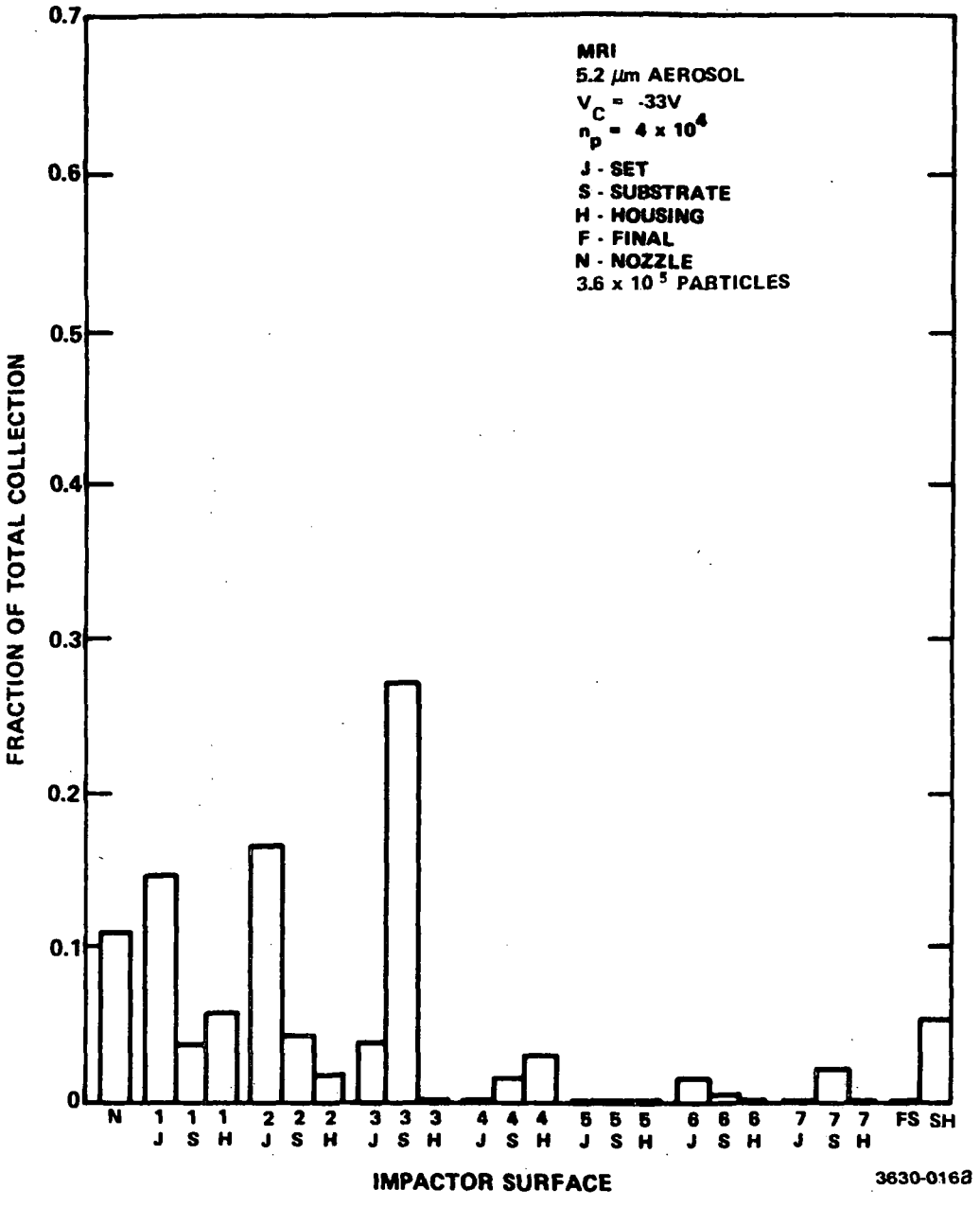

*Figure 8. **Sampling charged particles using MRI-Model 1502 Impactor with grounding** wire - high particle charge (See Figure 6 and 7 for comparison.)*

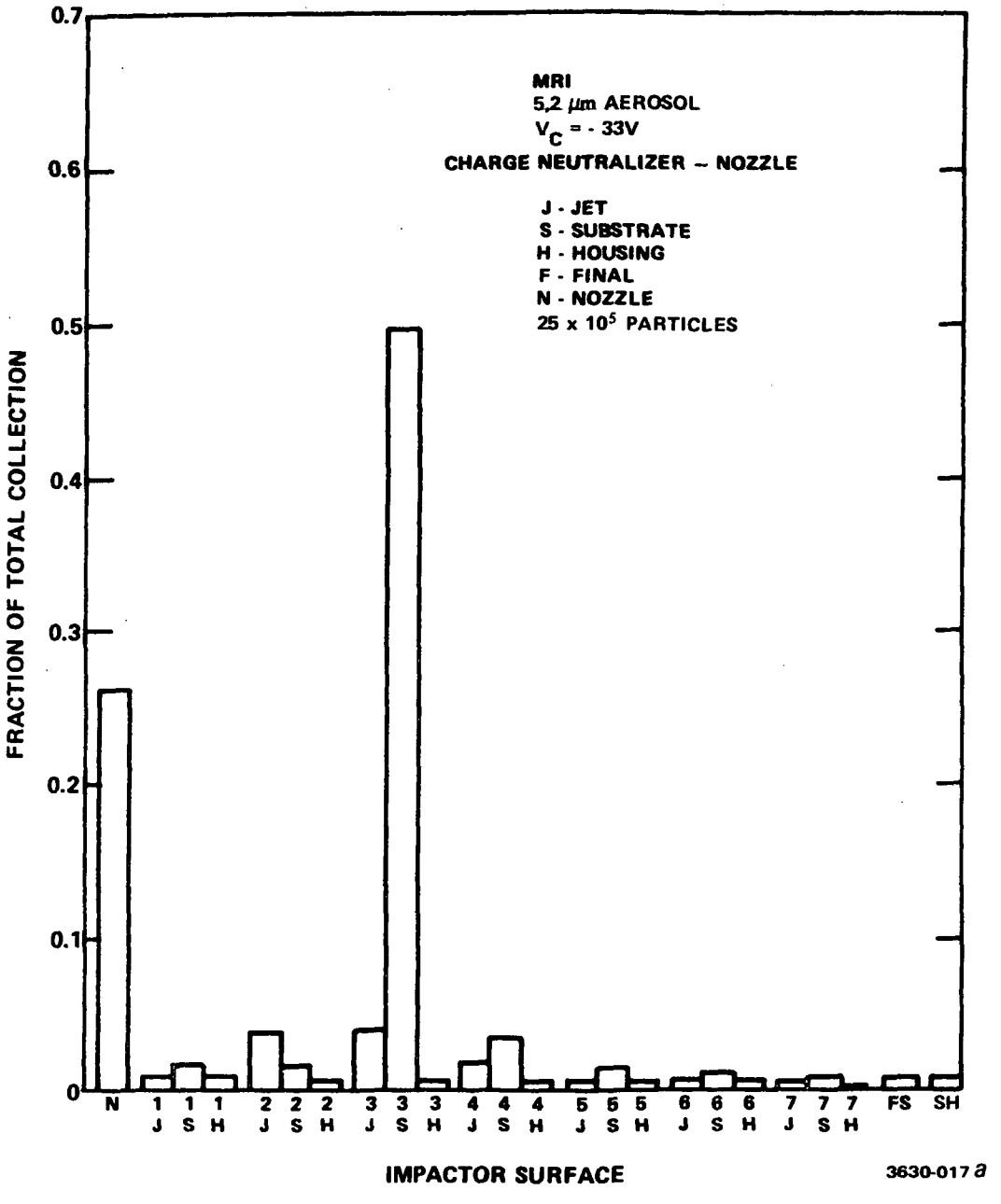

Figure 9. Sampling charge-neutralized particles using MRI-Model 1502 Impactor with neutralizer at nozzle - $n_p = 4 \times 10^4$.

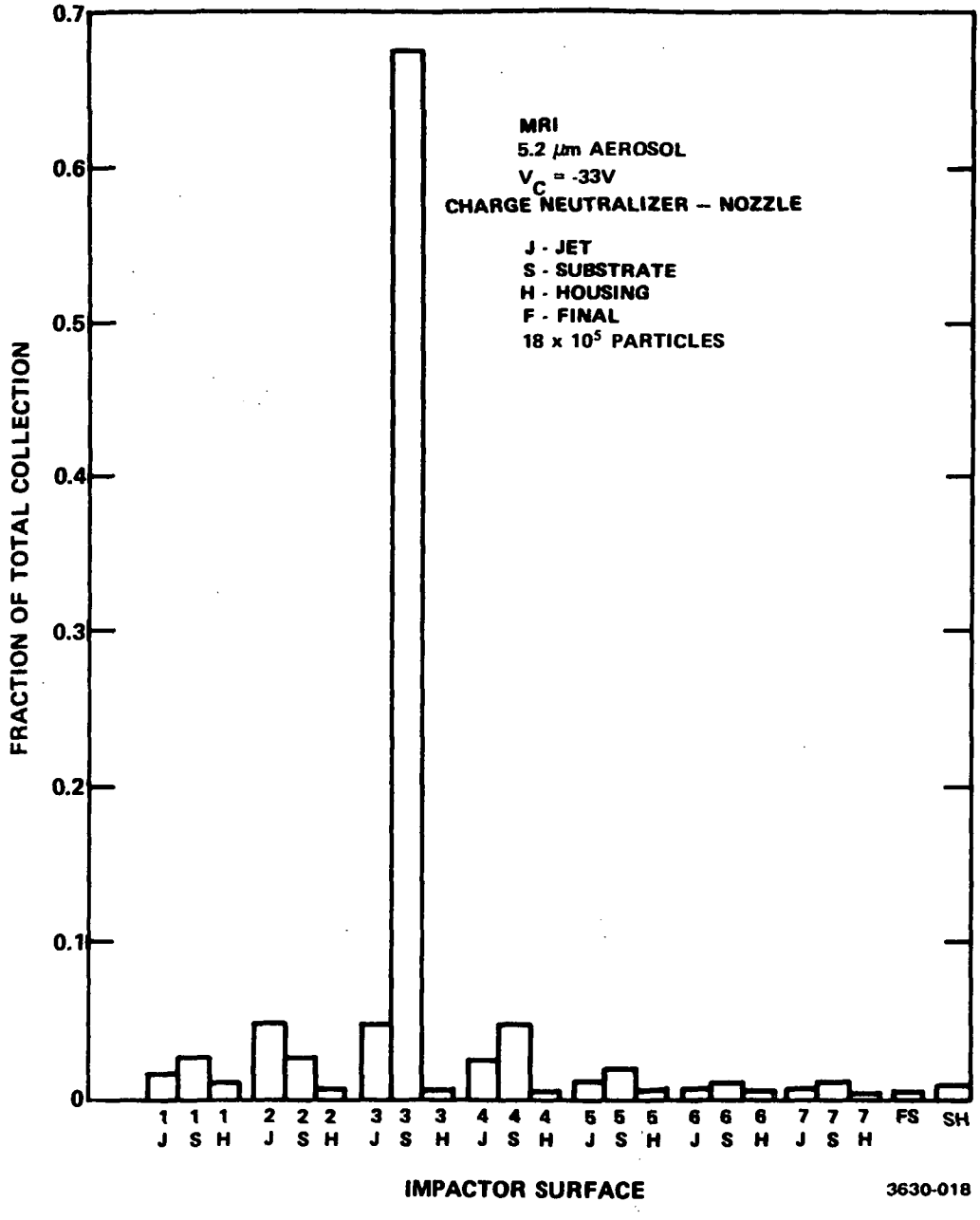

Figure 10. Sampling charge-neutralized particles using MRI-Model 1502 Impactor with nozzle losses corrected. (Run data identical to Figure 9.)

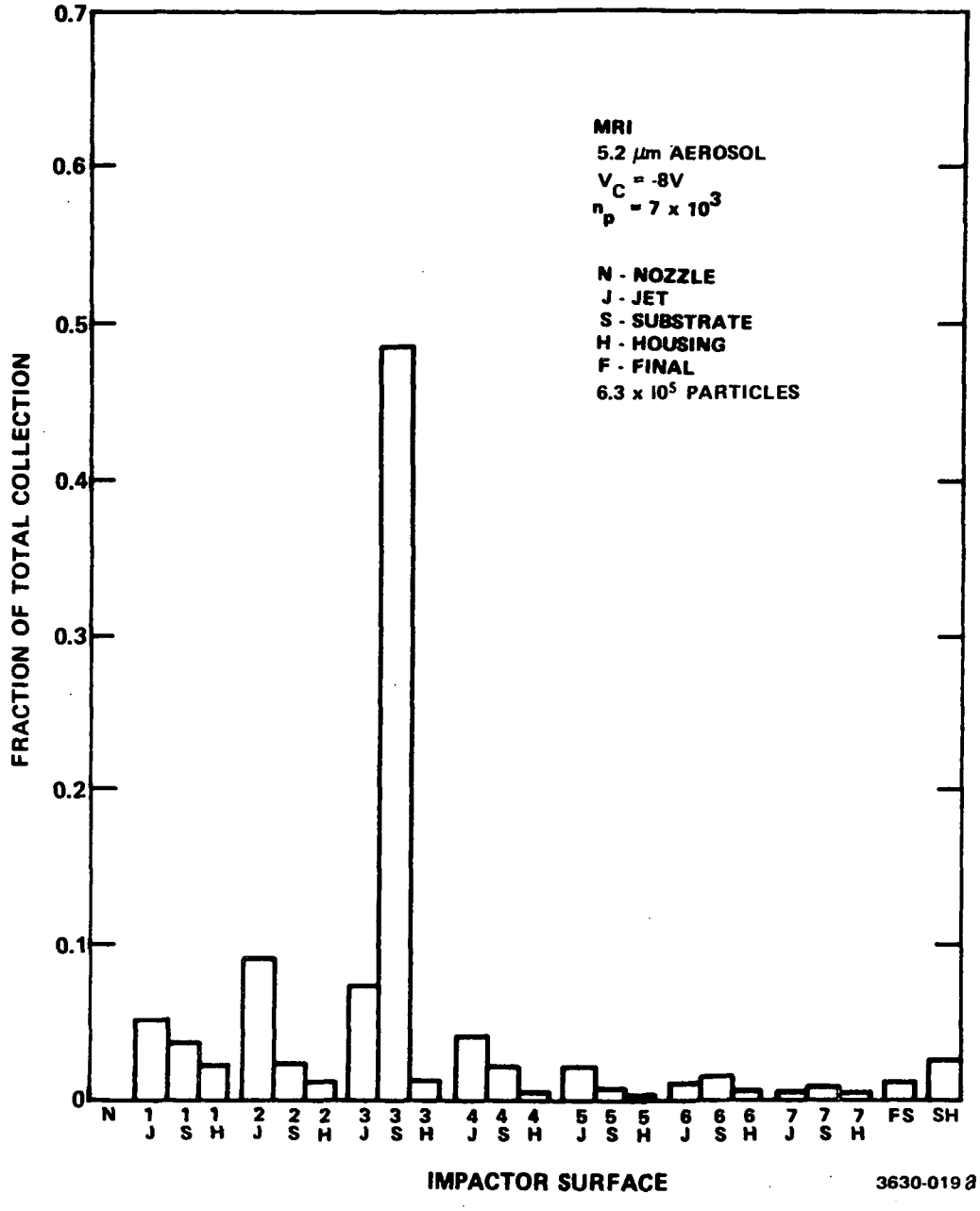

Figure 11. Sampling charged particles using MRI-Model 1502 Impactor with grounding wire-moderate particle charge. (See Figures 6 and 8 for comparison.)

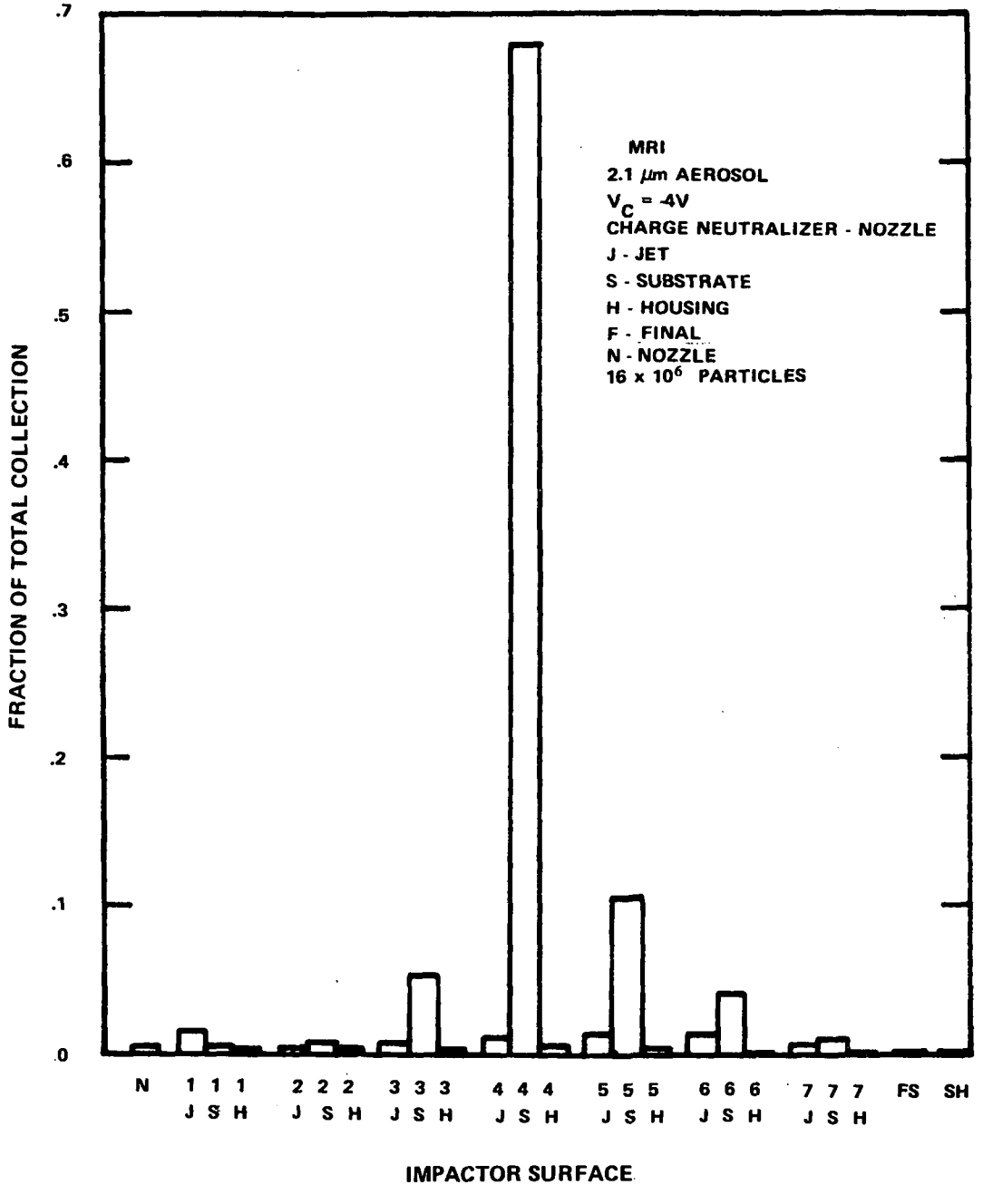

Figure 12. Sampling charge-neutralized particles using MRI-Model 1502 Impactor with neutralizer at nozzel -- n_D = 2.4 x 10^3. (See Figure 10 for comparison with 5.2 μm aerosol data.)

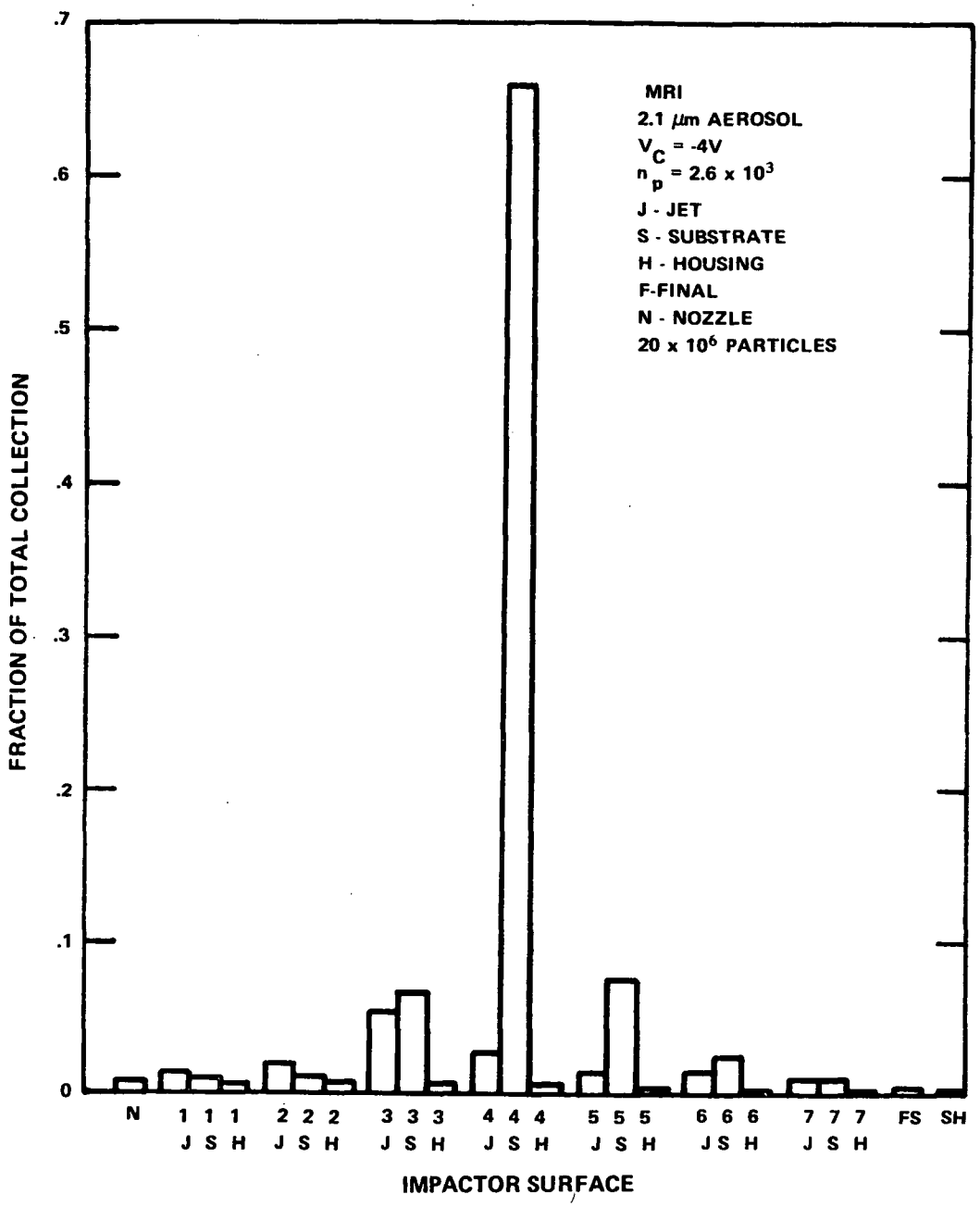

Figure 13. Sampling charged particles using MRI-Model 1502 Impactor with grounding wire - moderate particle charge. (See Figure 11 for comparision.)

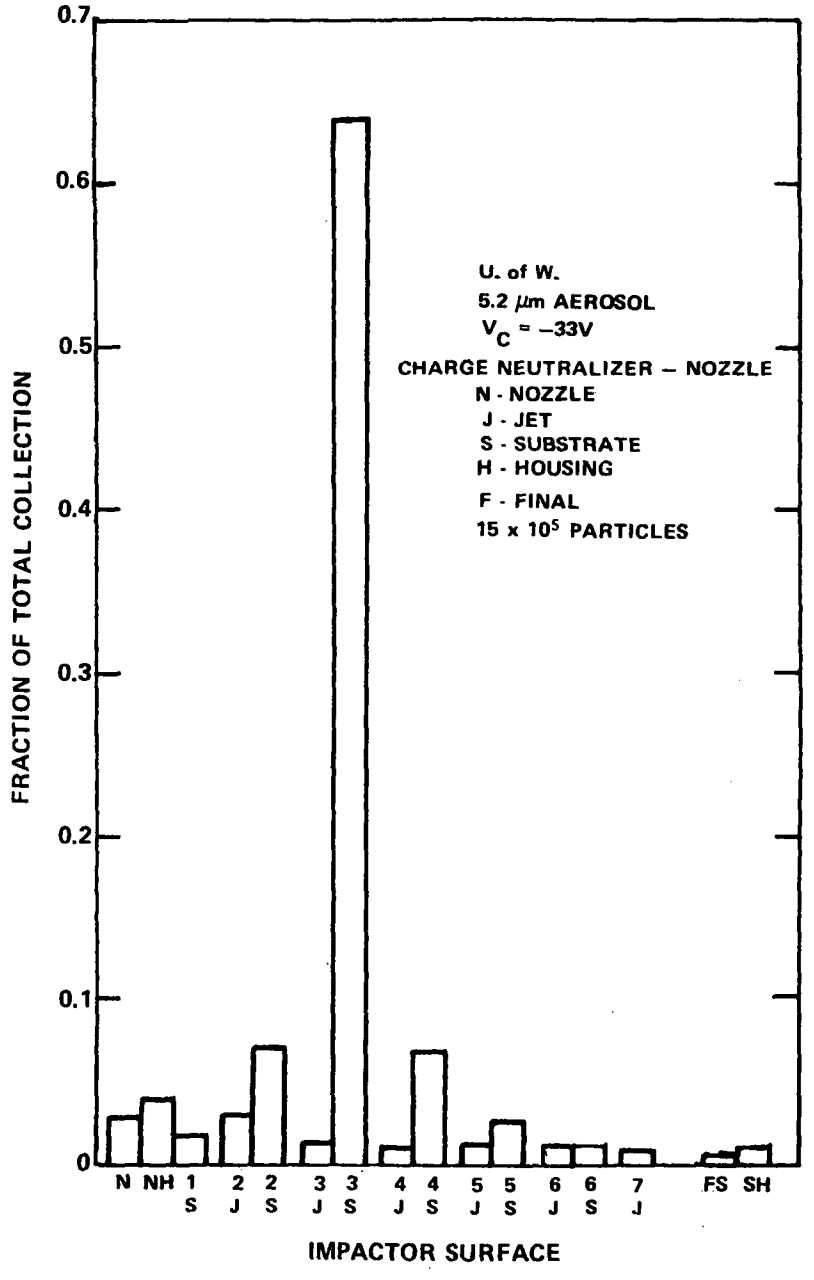

Figure 14. Sampling charge-neutralized particles using U. of W. Mark III Impactor with charge neutralizer at nozzle - $n_p = 4 \times 10^4$.

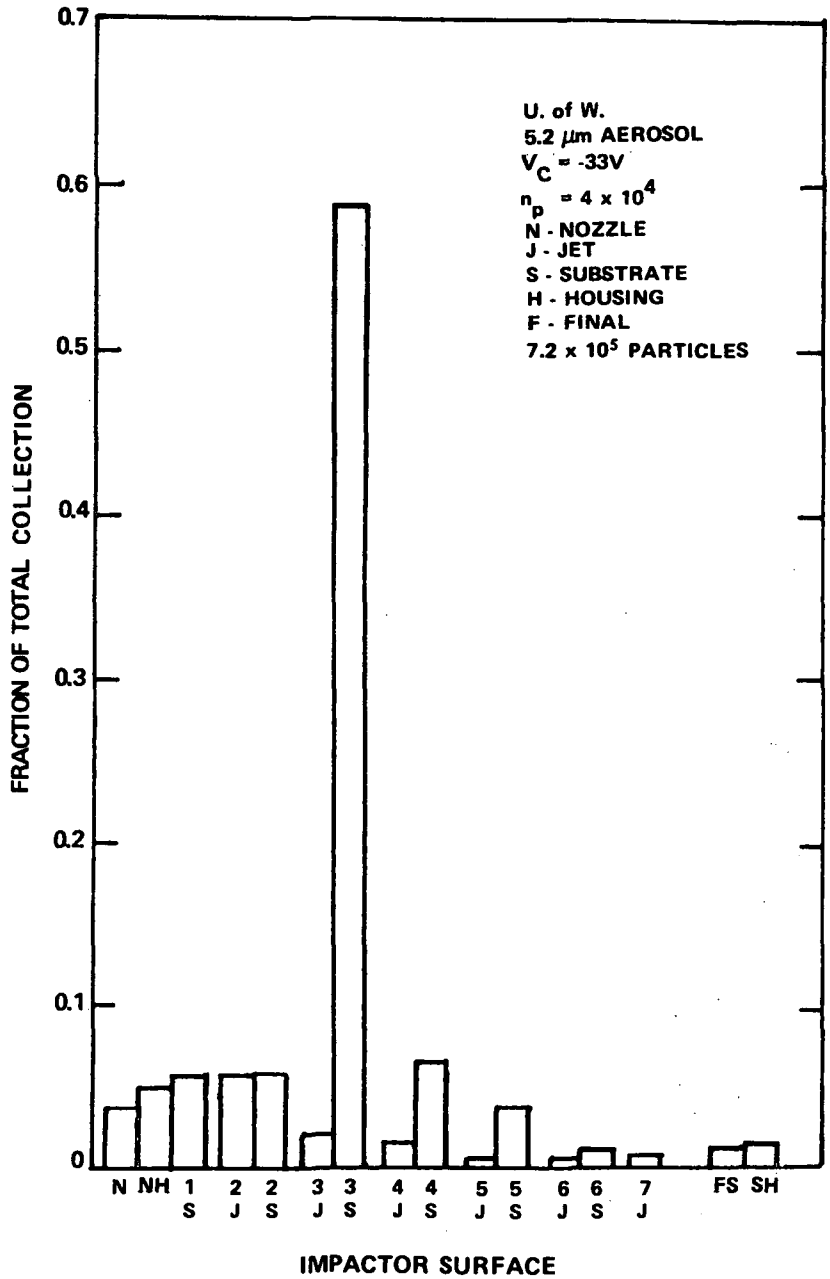

Figure 15. Sampling charged particles using U. of W. Mark III Impactor with no grounding wire - high particle charge. (See Figure 14 for comparison.)

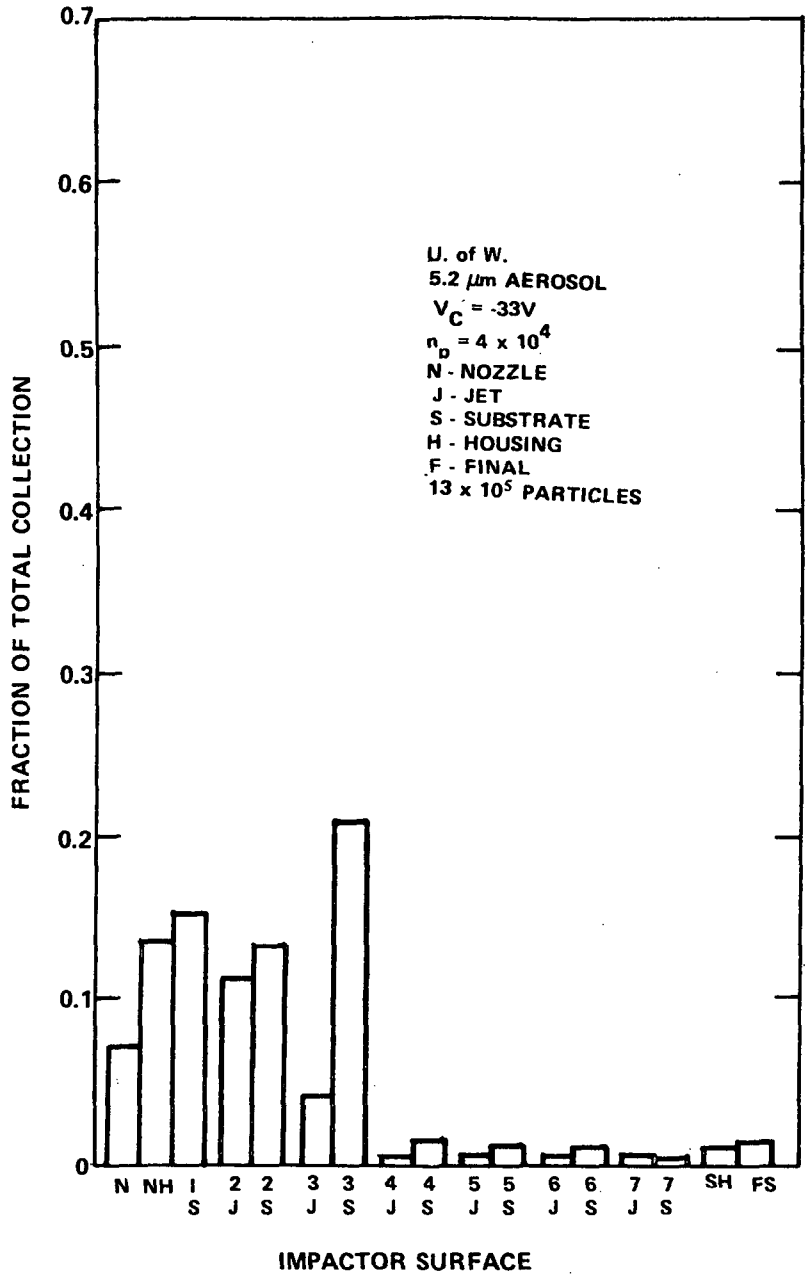

Figure 16. Sampling charged particles using U. of W. Mark III Impactor with grounding wire - high particle charge. (See Figures 14 and 15 for comparison.)

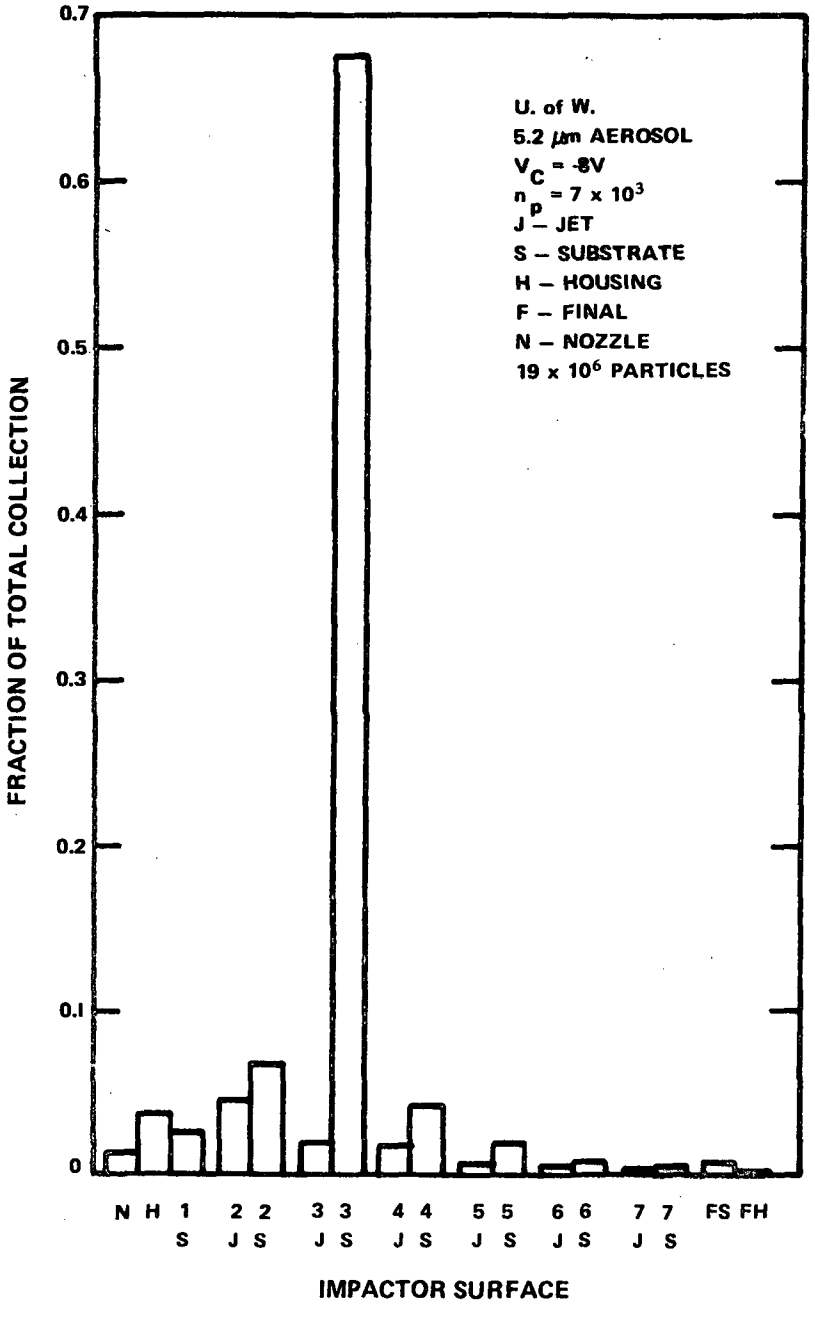

Figure 17. Sampling charged particles using U. of W. Mark III Impactor with grounding wire - moderate particle charge. (See Figures 14 and 16 for comparison.)

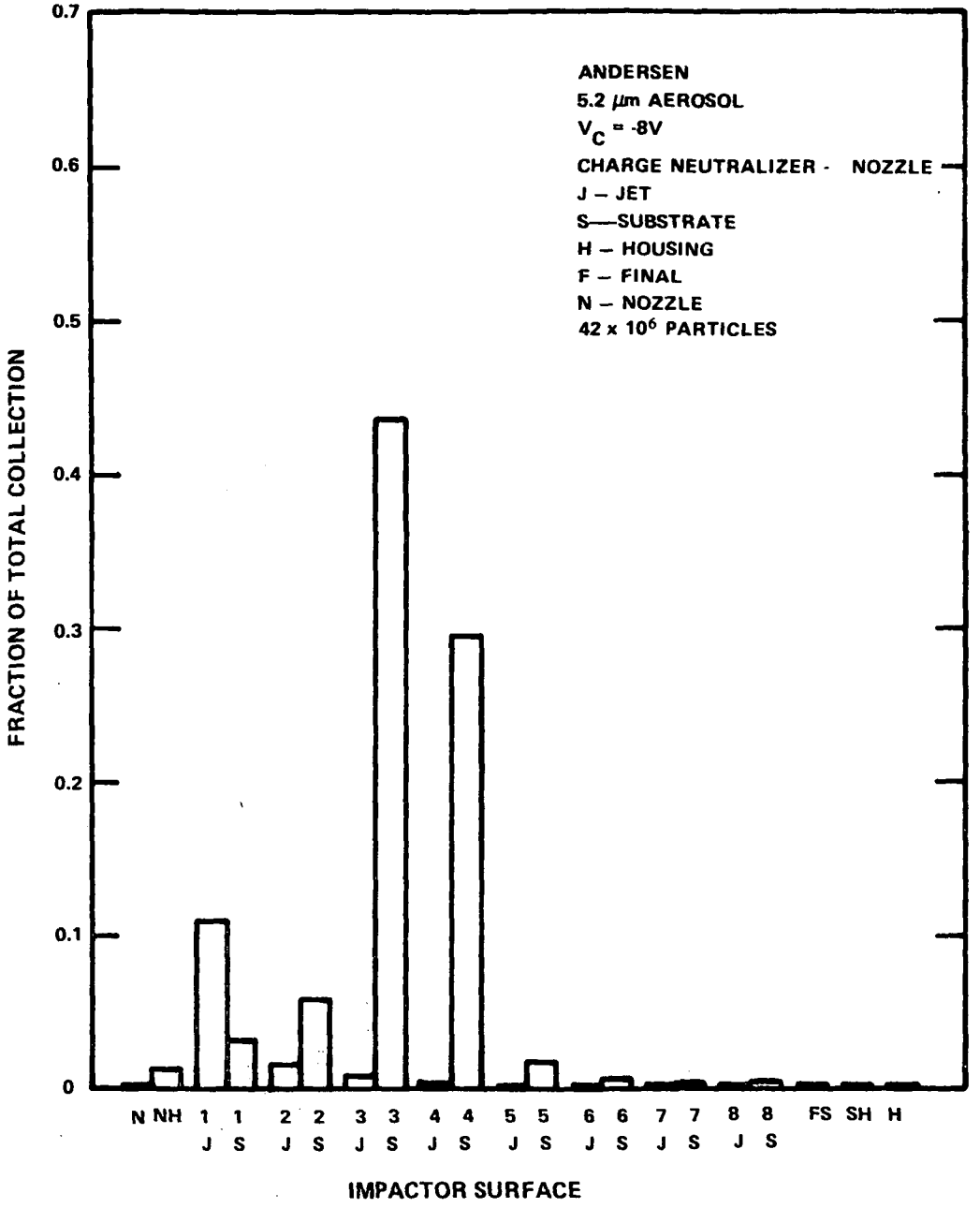

Figure 18. Sampling charge-neutralized particles using Andersen Mark III Stack Sampler with neutralizer at nozzle -- $n_D = 7 \times 10^3$.

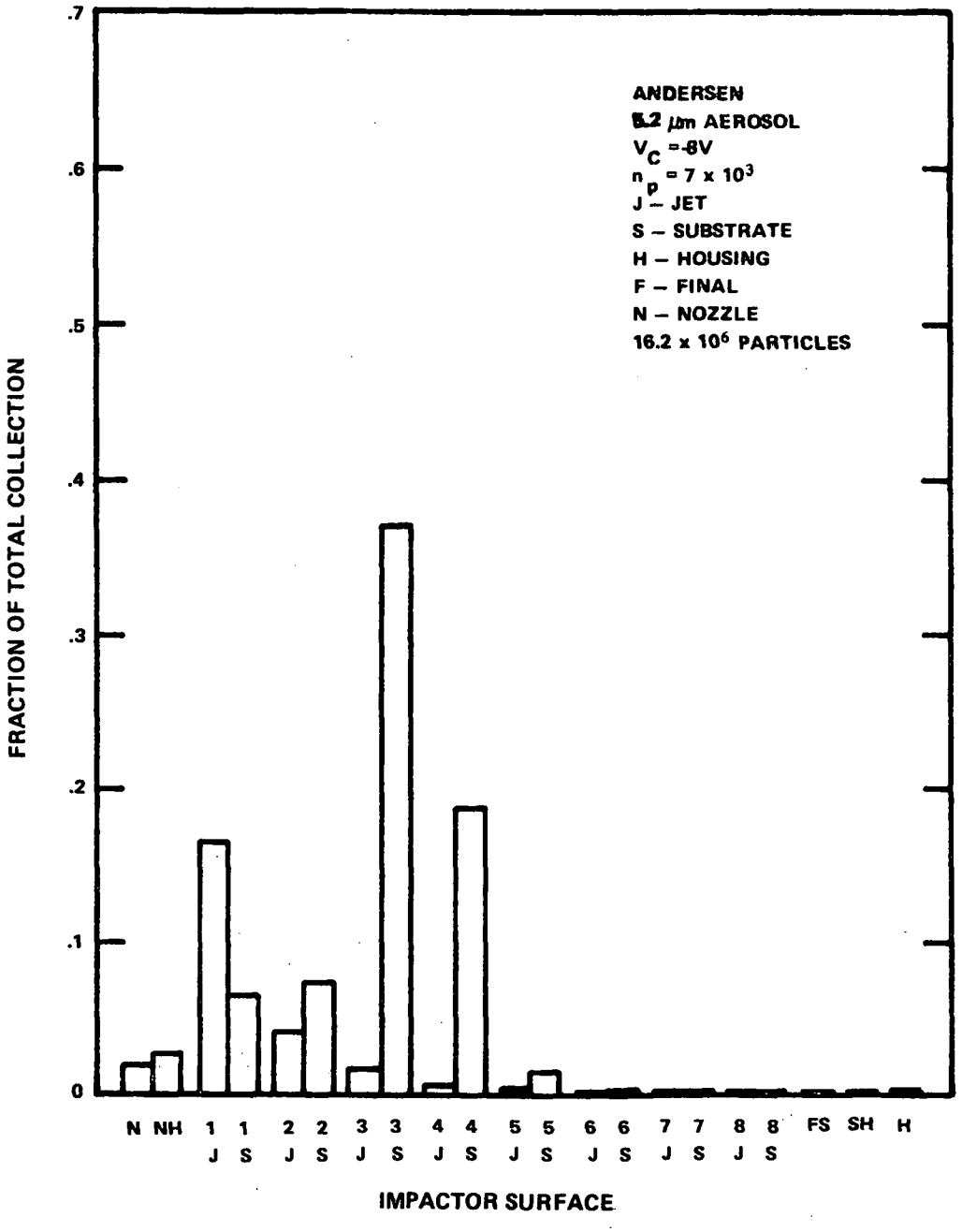

Figure 19. Sampling charged particles using Andersen Mark III Stack Sampler with grounding wire - moderate particle charge. (See Figure 18 for comparison.)

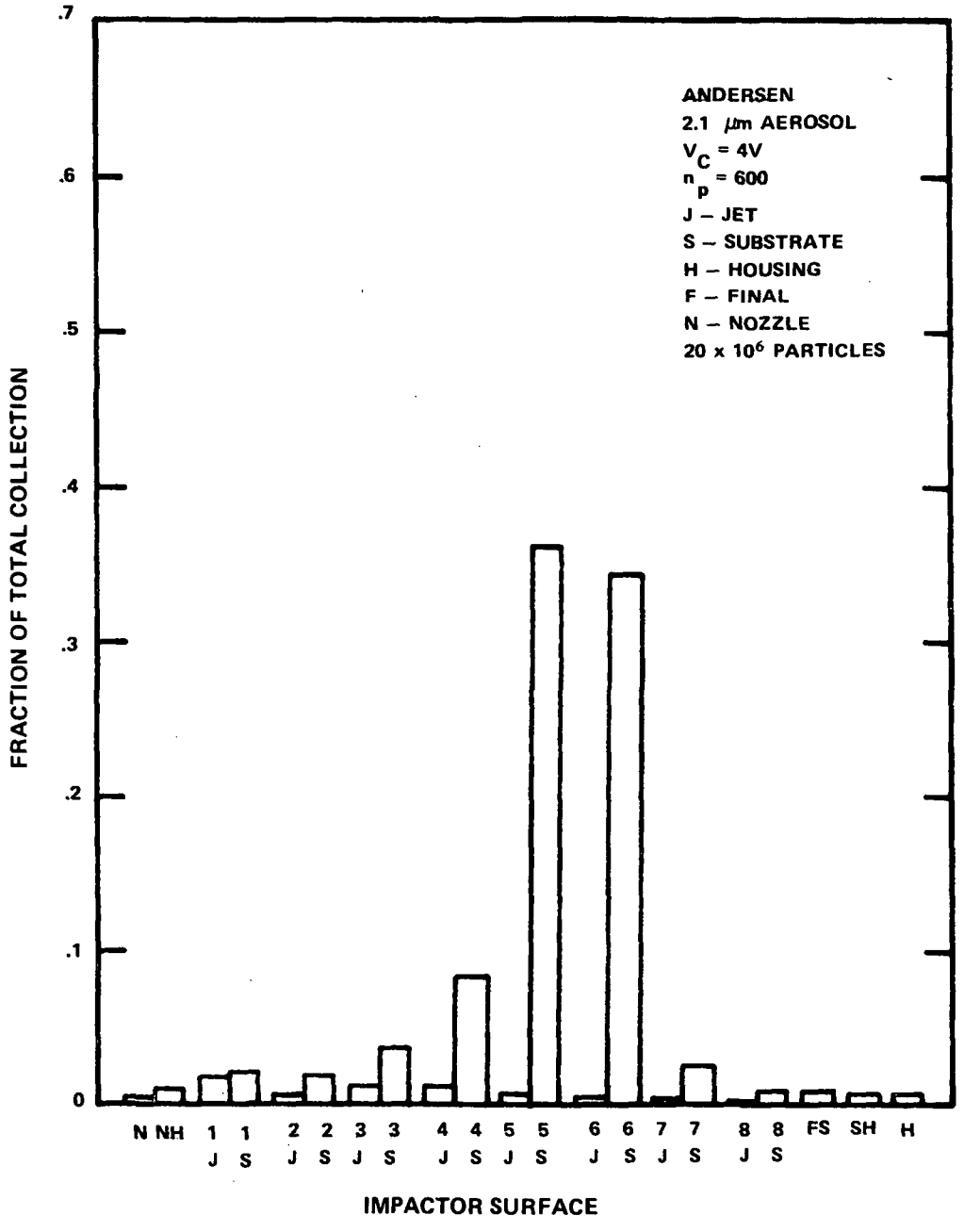

Figure 20. Sampling charged particles using Andersen Mark III Stack Sampler with grounding wire - moderate particle charge.

The data represented in Figure 8 were taken with the impactor electrically grounded, otherwise, the operating conditions were identical to those listed in Figure 7. The collection efficiencies of the nozzle and stage one jet plate (1J) are larger. Only the nozzle and 1J of the MRI were grounded from the outside due to an anodized coating on each stage housing. In these measurements a grounded wire was wrapped around the threads between 1J and its substrate housing. The resistances between ground and 1S and between ground and 2J were measured to be of the order of 10^9 ohms with the grounding wire and generally about 15% higher without the grounding wire.

Figure 9 presents a sampling run with identical operating conditions to that of Figure 8 except that a charge neutralizer was mounted upstream of the impactor nozzle. The neutralizer is a polonium 210 strip made by Nuclear Products Company. For use with an impactor it was bent to form a ring and placed at the entrance to the nozzle. In Figure 9 the high collection on the nozzle was thought to be a result of turbulence induced by the charge neutralizer. Collection efficiencies were calculated excluding the nozzle losses. These values are given in Figure 10. Comparing this figure to Figure 6 shows that indeed the effect of particle charge was eliminated by the ion source neutralizer. After this run the ionizer mount was changed to disturb the flow less.

Figures 7 and 8 showed an effect of high particle charge upon impactor behavior where the charge level was higher than encountered in most effluent streams. In the run depicted in Figure 11 the charge per particle was approximately 7×10^3 elementary charges, approximately the same as that expected in an industrial electrostatic precipitator. Collection by the stage 3 substrate (3S) was nearly twice that with 4×10^4 charges/particle (Figure 8) but was still 15% less than with no charge (Figure 6). These data indicate that in sampling 5.2 μm diameter particles exiting a precipitator, approximately 25% of the particles collect on surfaces

due to their charge and not size. This conclusion is based on the assumption that all particles exiting a precipitator have the level of charge predicted by Equation (1).

Figures 12 and 13 show the effect of moderate charge on 2.1 μm diameter particles. 3J and 4J again showed an increased collection when charged particles are sampled. However, the effect for 2.1 μm particles charged to saturation was much smaller than with the larger particles at saturation.

University of Washington Impactor

Figures 14 through 16 show data obtained from the University of Washington Mark III Impactor in sampling 5.2 μm diameter particles with 4×10^4 charges per particle. Figure 14 shows results with the charge neutralizer and Figures 15 and 16 without the neutralizer. The impactor was grounded electrically in the run depicted in Figure 16 and was not in Figure 15. Particle charge affected the collection efficiency of the various surfaces. The behavior of the U. of W. impactor was similar to that of the MRI impactor except that the use of a grounding lead produced a greater change in the deposition of charged particles for the U. of W. impactor.

The results obtained with the moderate charge level, 7×10^3 elementary charges, on 5.2 μm particles are shown in Figure 17. Comparison of these data with those in Figure 14 showed no significant effect on surface collection efficiency due to the increased charge level.

Andersen Impactor

Figures 18 and 19 show data obtained with the Andersen Mark III Stack Sampler when sampling 5.2 μm diameter particles with neutralized and moderate charge levels, respectively.

Comparison of these two figures showed a significant difference in the fraction of particles collected upstream of stages three and four. As with the MRI impactor about 25 percent of the 5.2 μm particles with moderate charge collected on wall and jet surfaces because of their charge rather than size.

Figure 20 shows sampling data for particles with 2.1 μm diameters and moderate charge, 600 elementary charges. The control run for this data, that is, the sampling of neutral particles with 2.1 μm diameters, had to be discarded because of an apparent syringe pump malfunction. However, the agreement of the data in Figure 20 with impactor theory for neutral particles and a previous sampling study[1] indicated that no significant effect of charge was present in sampling the 2.1 μm particles.

In the following section the data shown in Figures 6 through 20 are presented in terms of collection efficiency per stage versus Stokes number for different levels of charge.

Effect of Charge on Efficiency versus $\sqrt{\psi}$

Figures 6 through 20 depict impactor behavior under various circumstances involving particle charge. As discussed above, a high charge affected the deposition of particles. However, it is not clear from those figures to what extent charge altered the calculated size distribution in a collected sample.

The size distribution inferred from impactor data is based upon stage collection efficiency E_i as a function of the square root of inertial impaction parameter, $\sqrt{\psi}$.

$$\psi = D_p^2 C \rho_p V_o / 18 \eta D_j \qquad (11)$$

where D_p = particle diameter (cm),
C = Cunningham slip factor,
D_j = jet diameter (cm),
ρ_p = particle density (gm/cm^3),
η = gas viscosity (poise), and
V_o = jet velocity (cm/sec).

A representative example of efficiency versus $\sqrt{\psi}$ is given as a solid line in Figure 21. The use of E_i versus $\sqrt{\psi}$ gives the desired stage efficiency as a function of particle size for a range of sampling conditions. In practice a stage is calibrated by experimentally determining efficiency versus $\sqrt{\psi}$ for a particular substrate material to obtain $\sqrt{\psi_{50}}$; that is the value of $\sqrt{\psi}$ at 50% collection efficiency. Then, for particular sampling conditions the effective stage cut diameter D_{50} is obtained from $\sqrt{\psi_{50}}$. It is assumed that all particles caught by an impactor stage are those particles having diameters equal to or greater than the D_{50} of that stage, but less than the cut point of the preceding stage. Therefore, the effect of particle charge upon the calculated size distribution depends on its effect upon $\sqrt{\psi_{50}}$. More sophisticated deconvolution methods for impactor data which use the entire efficiency curves have been proposed[5,6,7], but use of these techniques is limited to low-noise sampling data.

In order to completely characterize the effect of particle charge, the function $E_i(\sqrt{\psi}, n_p)$ [that is, efficiency expressed as a function of the square root of the Stokes number and charge n_p for stage i] is required. For neutral aerosols, $E_i(\sqrt{\psi}, 0)$ has been determined in an extensive calibration study[1] for each stage of the Andersen, MRI, and Univ. of Washington impactors at

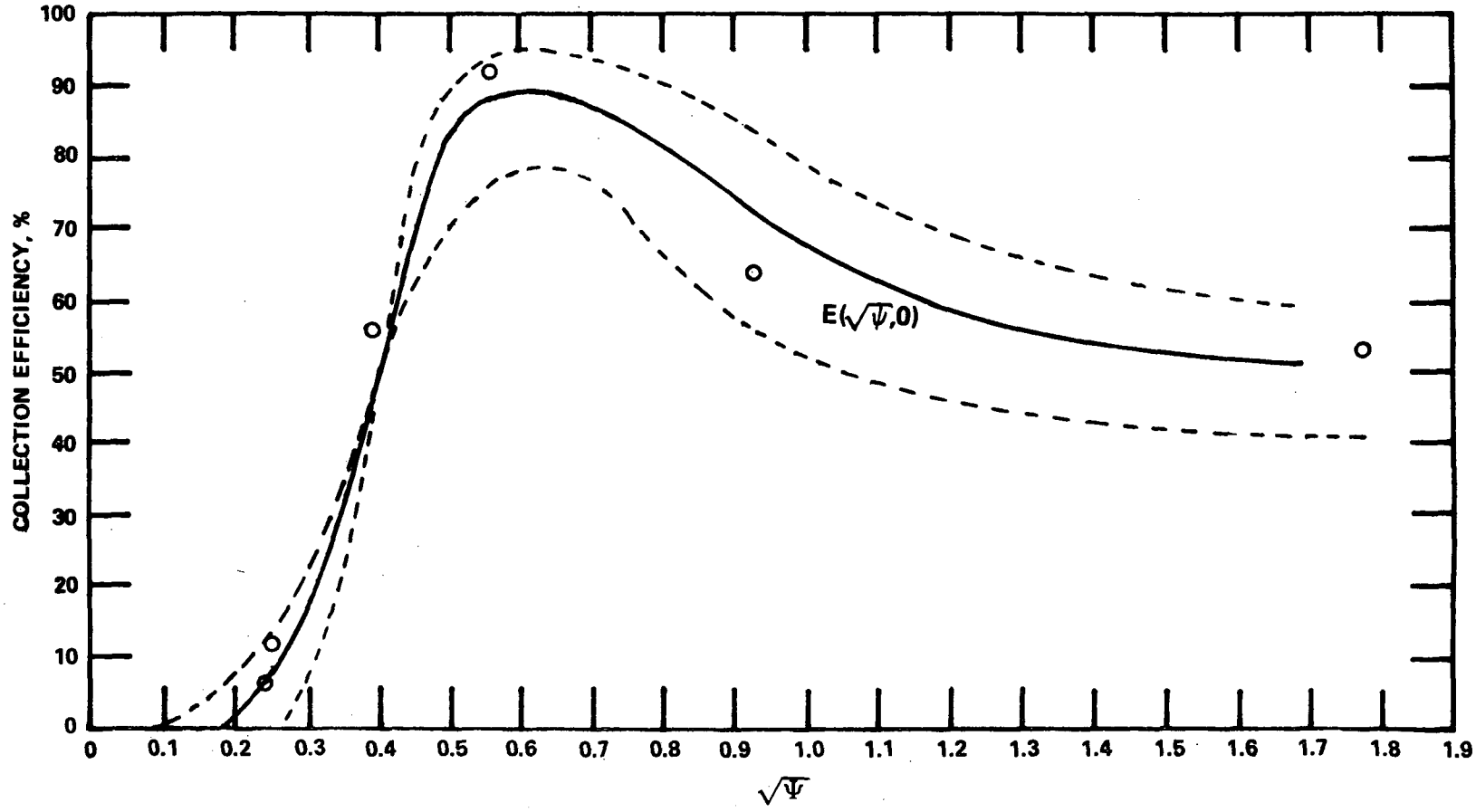

Figure 21. Reference curve (solid) giving collection efficiency as a function of $\sqrt{\Psi}$ for the Andersen Stack Sampler and neutral particles. The measurements ("O") of this study for neutral particles are plotted by the procedure given in the text. The dashed lines depict the envelope of all stage efficiency curves superimposed.

the sampling conditions used here, except that grease substrates were used with the latter two. To a first approximation, $E_i(\sqrt{\psi},0)$ has the same form for all stages with the same substrate material and impactor. The reference curve which we denote by $E(\sqrt{\psi},0)$ in Figure 21 was drawn by superimposing the stage calibration curves of the Andersen from the previous study.[1] Since the major differences in $E_i(\sqrt{\psi},0)$ from one stage to another is not in the shape of the curve, but $\sqrt{\psi_{50}}$, for the purpose of this analysis the calibration curves were normalized so that $\sqrt{\psi_{50}}$ of each coincided at 0.4. The dashed lines in Figure 27 define the envelope of those curves.

The collection efficiency of each stage was calculated for each run from the data given in Figures 6 through 20. These efficiencies were "corrected for wall losses" by combining the particles collected on the various surfaces according to Table II. These groupings are based upon the procedure used in field testing and the laboratory observations discussed above concerning deposition on jet plates. In the field, particulate mass on the top of jet plates is combined with the preceding stage, and that on the bottom is combined with the stage below the jet plate. The results for sampling neutral particles with the Andersen are given in Figure 21 as points. For comparison of these data to our reference curve, each measured efficiency is normalized and plotted as described above. The deviations of the data points from the reference curve in Figure 21 is thus a measure of the degree to which impactor calibration data for neutral particles may vary. In Figure 22 the same procedure was followed to relate the measured efficiencies of the Andersen stages with charged particles to its generalized efficiency curve for neutral particles. The dashed curve is the resulting $E(\sqrt{\psi},n_p)$ for moderate n_p. The effect of charge was to reduce the sharpness (slope) of the curve at $\sqrt{\psi}$ values below the peak while not changing $\sqrt{\psi_{50}}$ significantly. At $\sqrt{\psi}$ values above the peak the effect of charge was to reduce the efficiency in a manner similar to particle bounce effects.

Table II . Grouping of Surfaces for the Efficiency of Each Impactor Stage.

Stage	Andersen surface	MRI surface	U. of W. surface
1	N NH 1J 1S 2J	N 1J 1S 1H	N NH 1S
2	2S 3J	2J 2S 2H	2J 2S
3	2S 4J	3J 3S 3H	3J 3S
4	4S 5J	4J 4S 4H	4J 4S
5	5S 6J	5J 5S 5H	5J 5S
6	6S 7J	6J 6S 6H	6J 6S
7	7S 8J	7J 7S 7H FS SH	7J 7S FS SH
8	8S FS SH H		

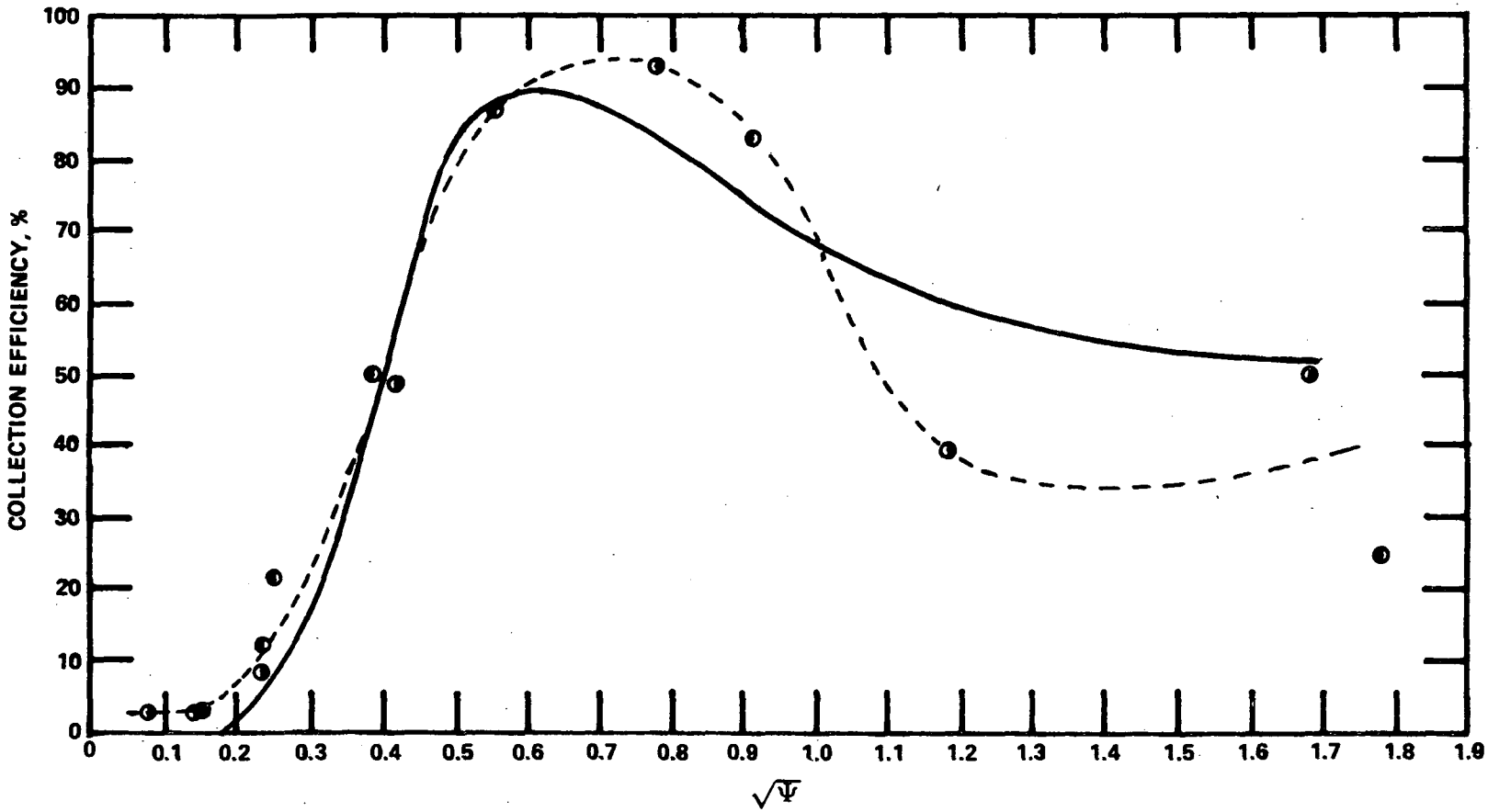

Figure 22. Efficiency versus $\sqrt{\Psi}$ of stages in Andersen Stack Sampler for neutral particles (solid curve) and moderately charged particles (dashed curve). The measurements of this study for moderately charged particles ("●" - 5.2 μm and "●" - 2.1 μm diameter) are plotted by the procedure given in the text.

Figures 23 and 24, and Figures 25 and 26 present information about the MRI and Univ. of Washington impactors analogous to that in Figures 21 and 22 for the Andersen. Stage efficiency curves of the previous study[1] for neutral particles were obtained using grease rather than glass fiber substrates; therefore some adjustments in the reference curves had to be made based upon the efficiency data of the present study and comparisons of available efficiencies of another impactor with these two substrates to determine the differences. The resulting reference curve of the MRI impactor is shown in Figure 23. For $\sqrt{\psi}$ values up to 0.5, following the same procedure as in Figure 21, the reference curve of Figure 23 was obtained using MRI efficiency curves for grease substrates. The use of these was justified because, in this region, the efficiencies for neutral particles measured in this study did not substantially deviate from this reference curve.

In the region of $\sqrt{\psi}$ values greater than 0.5, glass fiber substrates produced substantial bounce, meaning that efficiency dropped to much less than 100%. This is indicated by the low measured efficiencies shown in Figure 23. Therefore in this region a reference curve was determined from experimental data for neutral particles taken in the course of this study.

Figure 24 shows the effect of high and moderate particle charge upon the MRI stage efficiency versus $\sqrt{\psi}$. For moderate charge the effects were similar to those for the Andersen. At the higher charge level, however, the changes in $E(\sqrt{\psi},n_p)$ were quite large at all $\sqrt{\psi}$ values.

The effect of particle charge upon Univ. of Washington stage efficiency, shown in Figure 26, was small for moderate charge and substantial for high charge. In the "bounce" region, moderate charge appears to increase the efficiency substantially, thus reducing the effects of bounce. However, data obtained for $\sqrt{\psi}$ values to the right of the peak in efficiency are inherently

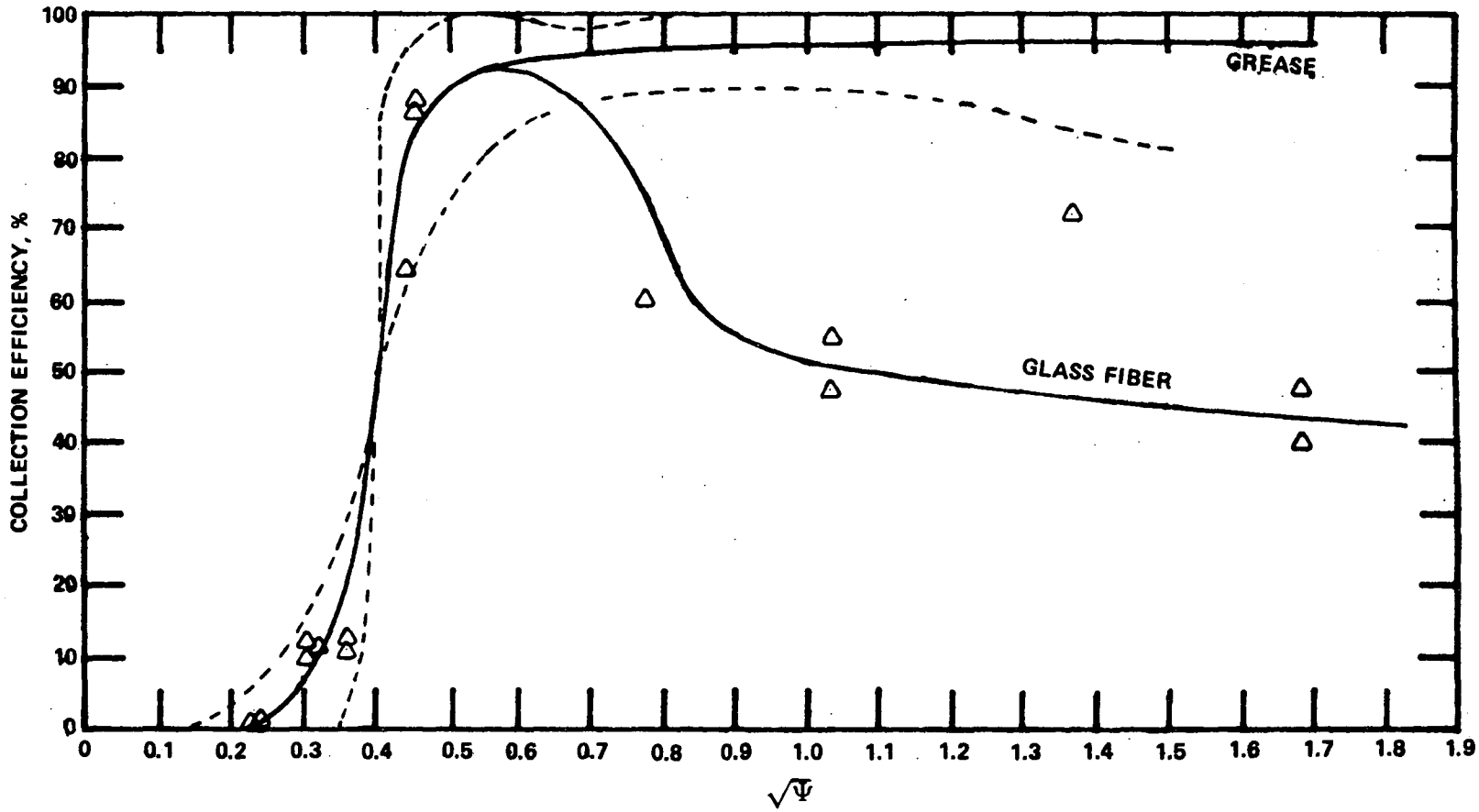

Figure 23. Reference curve (solid) giving collection efficiency as a function of $\sqrt{\Psi}$ for the MRI-Model 1502 Impactor and neutral particles. The measurements ("Δ") of this study for neutral particles are plotted by the procedure given in the text. The dashed lines depict the envelope of all stage efficiency curves superimposed.

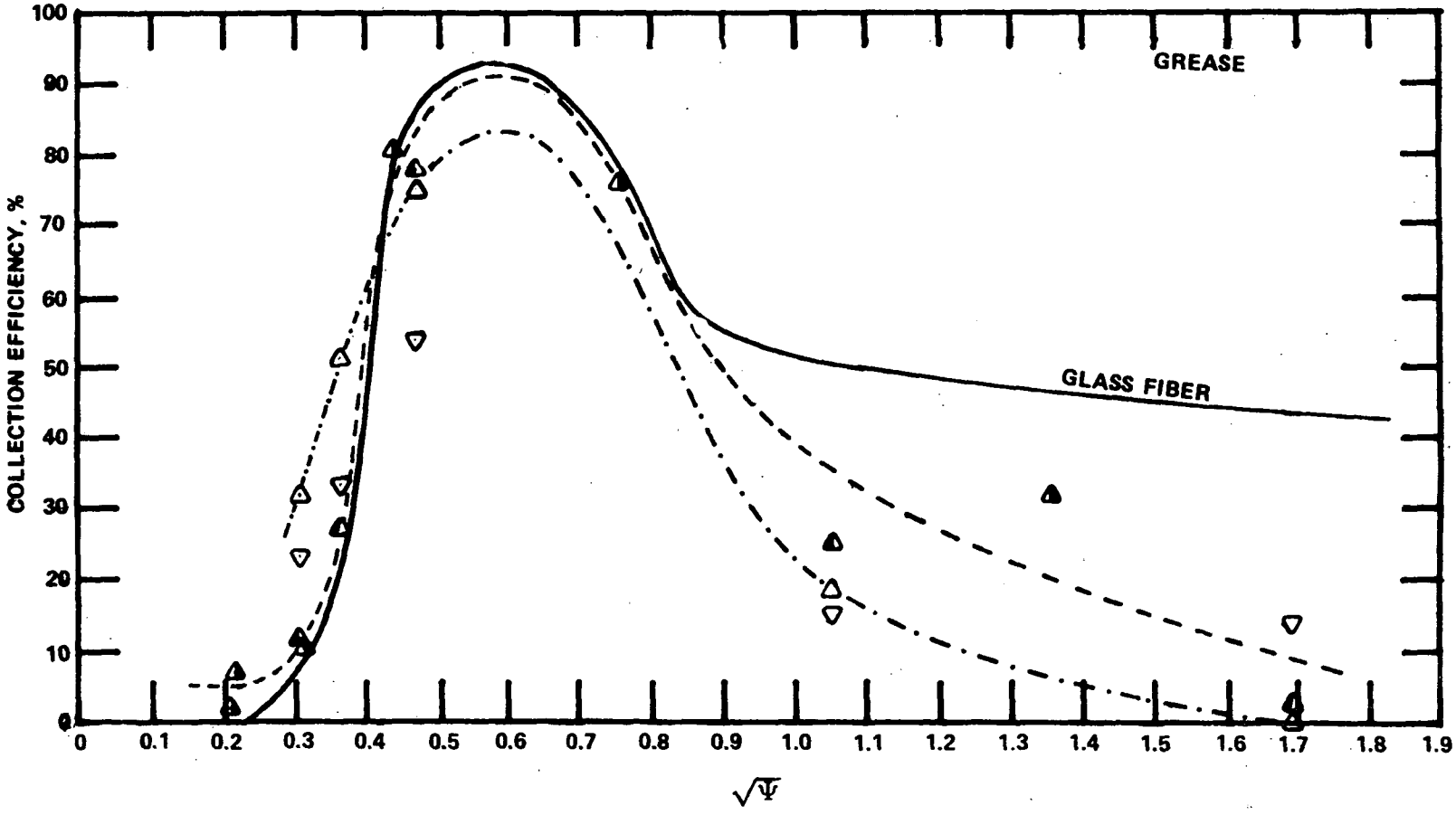

Figure 24. Efficiency versus $\sqrt{\Psi}$ of stages in MRI-Model 1502 Impactor for neutral (solid curve), moderately charged (dashed curve), and highly charged (-·-·-) particles. The measurements of this study for moderately charged ("▲" - 5.2 μm and "▲" - 2.1 μm diameters) and highly charged 5.2 μm diameter ("△" - grounded and "▽" - not grounded) particles are plotted by the procedure given in the text.

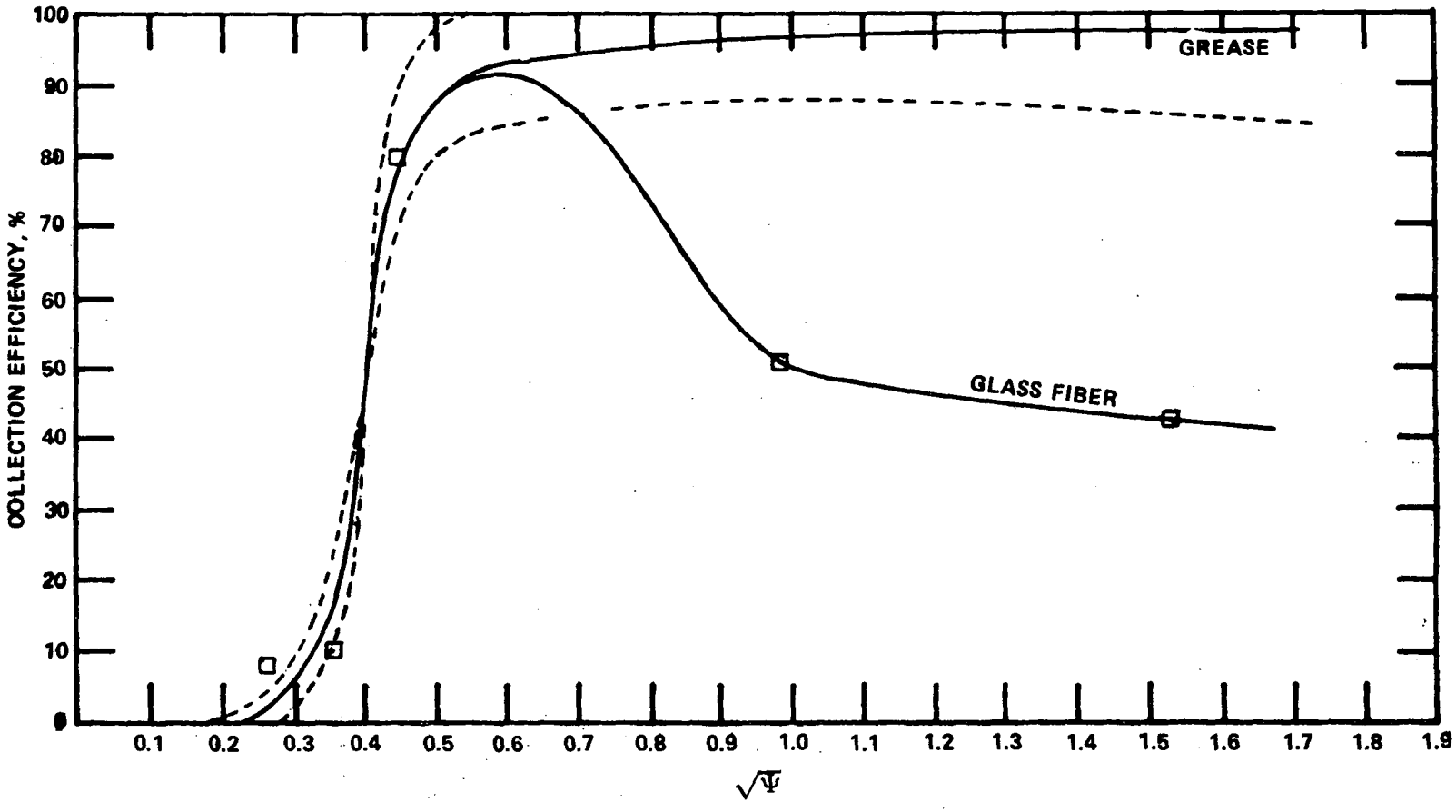

Figure 25. Reference curve (solid) giving collection efficiency as a function of the $\sqrt{\Psi}$ for the U. of W. Mark III Impactor and neutral particles. The measurements ("□") of this study for neutral particles are plotted by the procedure given in the text. The dashed lines depicted the envelope of all stage efficiency curves superimposed.

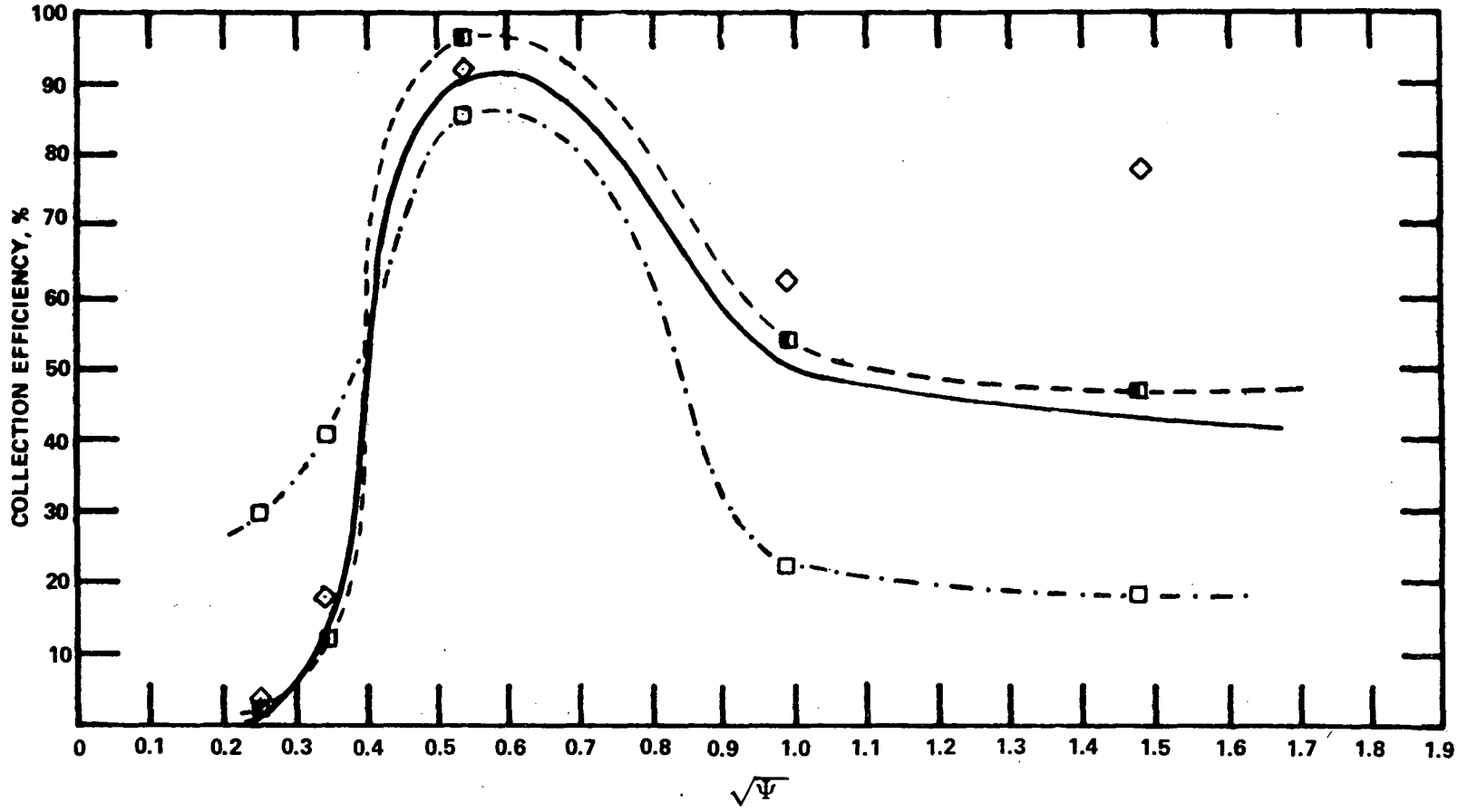

Figure 26. Efficiency versus $\sqrt{\Psi}$ of stages in the U. of W. Mark III Impactor for neutral (solid curve), moderately charged (dashed curve), and highly charged (-·-·-) particles. The measurements of this study for 5.2 μm diameter particles, moderately charged ("◧") and highly charged ("□" - grounded and "◇" not grounded) are plotted by the procedure given in the text.

subject to fluctuation because small numbers of particles are involved. Therefore, exceptions to the overall trends in this region are questionable.

Figures 22, 24, and 25 show two obvious effects of particle charge. At low values of $\sqrt{\psi}$ the stage efficiency was increased due to the collection of particles on metal jet plates. At high values of $\sqrt{\psi}$, past the peak, the efficiency was reduced as if repulsive forces of charge were significant. Charge produced very small changes in D_{50}.

Particle Deposition Patterns

The deposition patterns of fluorescein particles on impactor surfaces were observed by spraying them with a water mist and exposing them to a fluorescent light.

Photographs in Figures 27 and 28 show representative deposition patterns of particles on the top and bottom of jet plates and on substrates in the MRI impactor. Most particles deposited on the jet plates were on the bottom or downstream side of the plate as shown in these photographs. This pattern was visible with both charged and uncharged particles, but more particles were deposited on the bottom of the plates in the charged case. Apparently, particles passed in the vicinity of these surfaces whether charged or not. As expected, the Univ. of Washington impactor, with a similar geometry, had deposition patterns similar to those on the MRI.

Collection efficiencies of jet plates in the Andersen impactor were also slightly higher for charged particles than for neutral ones. Also, substantial numbers of charged particles were observed to be deposited on the upper surface around jets as well as on the bottom surface. The photographs in Figures 29-31 illustrate the Andersen deposition data.

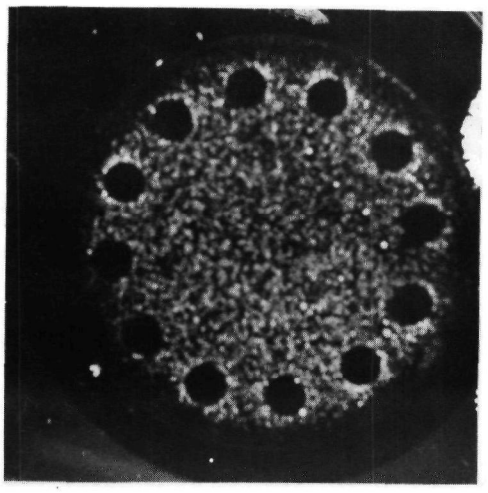

FRONT OF SECOND JET PLATE

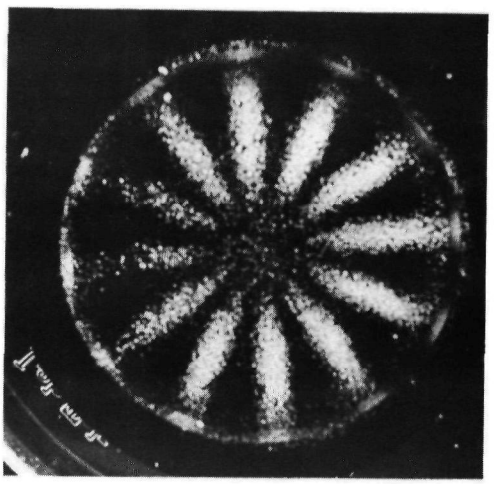

BACK OF SECOND JET PLATE

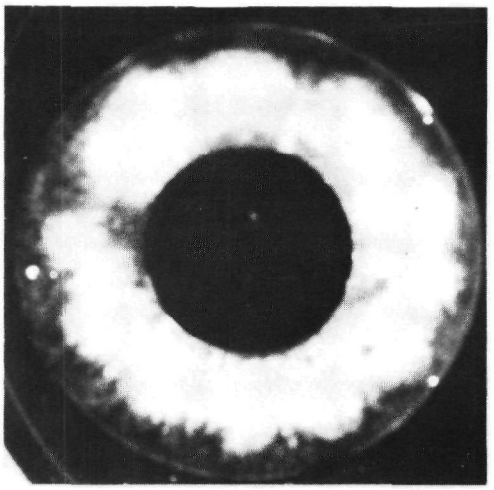

SECOND SUBSTRATE

3630-024

Figure 27. Photographs of deposition patterns of ammonium fluorescein particles in MRI-Model 1502 Impactor. Particle diameter was 5.2 μm. Sampling test data are in Figure 8.

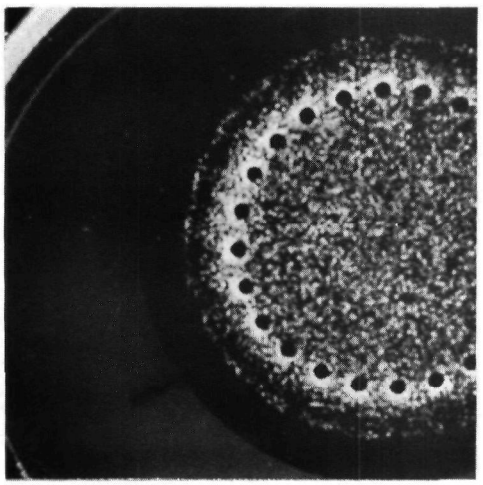

FRONT OF THIRD JET PLATE

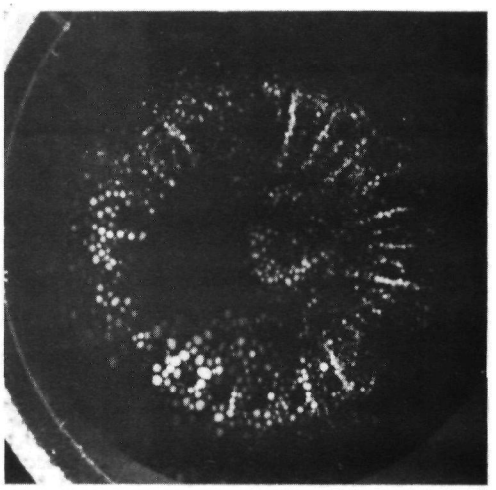

BACK OF THIRD JET PLATE

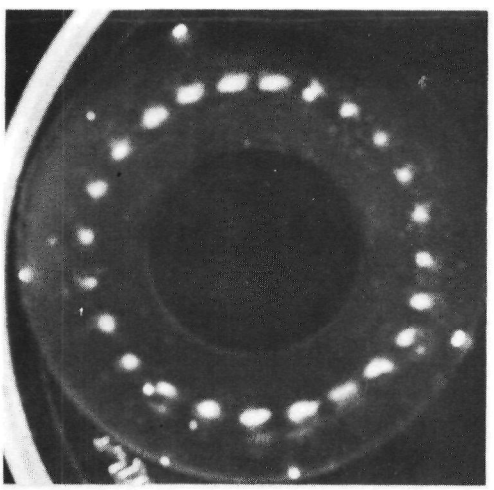

THIRD SUBSTRATE

3630-023

Figure 28. Photographs of deposition patterns of ammonium fluorescein particles in MRI-Model 1502 Impactor. Particle diameter was 5.2 µm. Sampling test data are in Figure 8.

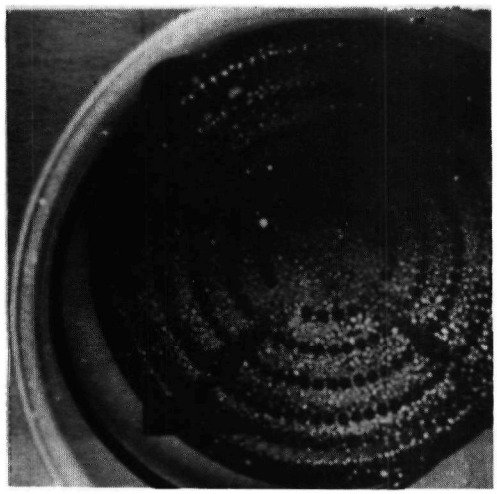

FRONT OF FIRST JET PLATE

BACK OF FIRST JET PLATE

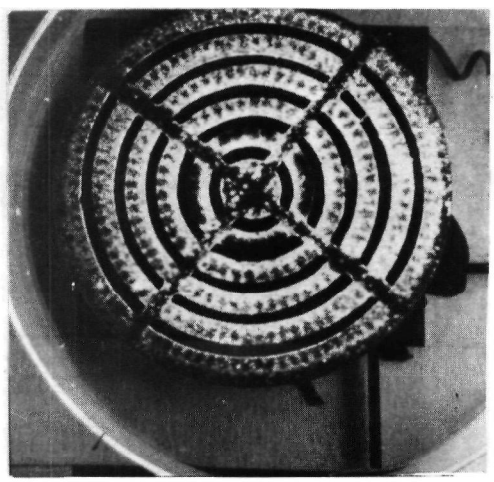

FIRST SUBSTRATE

Figure 29. Photographs of deposition patterns of ammonium fluorescein particles in Andersen Mark III Stack Sampler. Particle diameter was 5.2 μm. Sampling test data are in Figure 19.

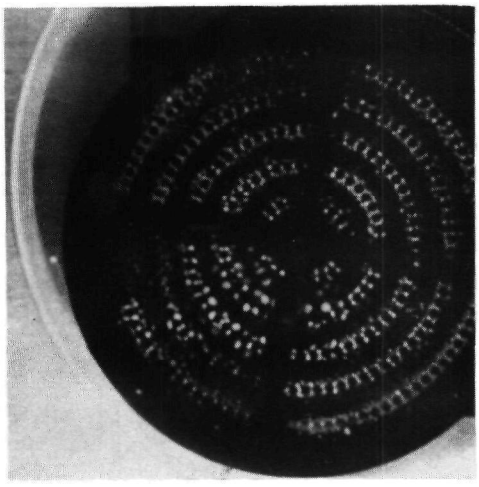

FRONT OF SECOND JET PLATE

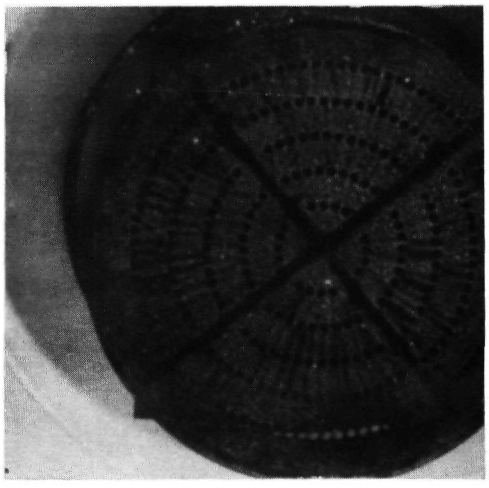

BACK OF SECOND JET PLATE

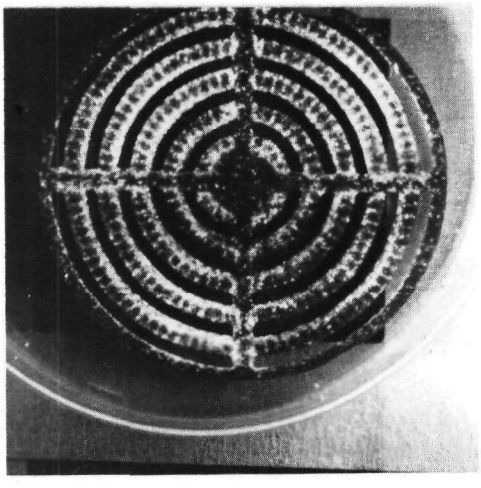

SECOND SUBSTRATE

Figure 30. Photographs of deposition patterns of ammonium fluorescein particles in Andersen Mark III Stack Sampler. Particle diameter was 5.2 µm. Sampling test data are in Figure 19.

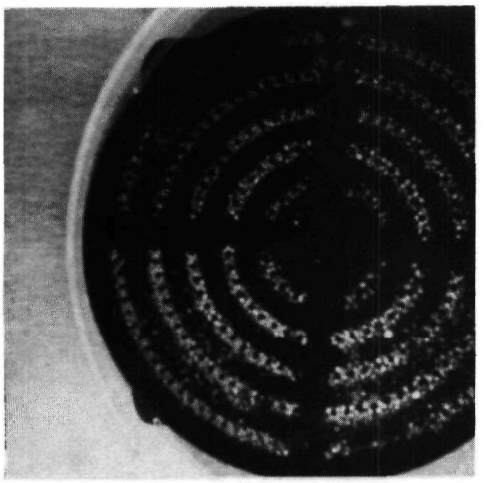

FRONT OF THIRD JET PLATE

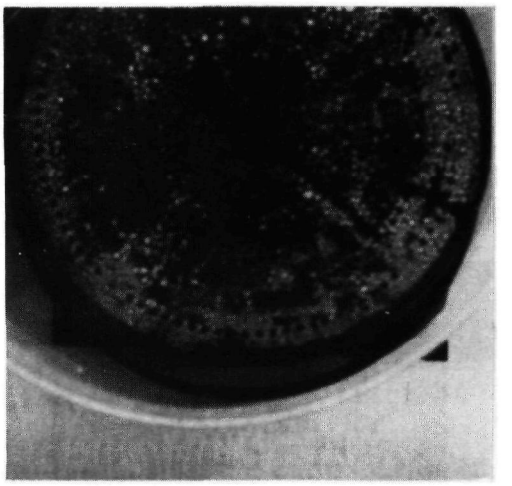

BACK OF THIRD JET PLATE

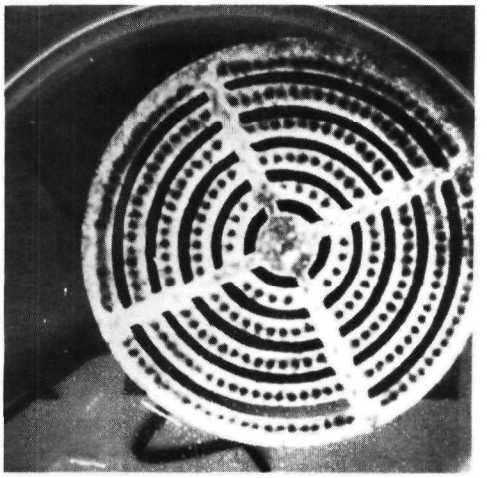

THIRD SUBSTRATE

Figure 31. Photographs of deposition patterns of ammonium fluorescein particles in Andersen Mark III Stack Sampler. Particle diameter was 5.2 μm. Sampling test data are in Figure 19.

Nonconducting Jet Plates

In an effort to study the effect that jet plates made from an insulated material would have on deposition due to particulate charge, plates 2J, 3J, and 4J were fabricated of plexiglass for the MRI impactor in an attempt to eliminate the effect. The data for this experiment are shown in Figure 32. Comparison with Figures 6 and 11 revealed two significant differences. First, the stage cut points are shifted to larger sizes. The origin of this behavior is not known (measurements ruled out changes in jet hole sizes as a source of discrepancy). Secondly, the collection efficiencies of 2J, 3J, and 4J were reduced, but the efficiencies of the nozzle, 1J, 1S, 1H, and especially 2S were increased. The reason the efficiency of 2S is so great might be attributed to the presence of static charges on 2J. It is unknown why the efficiencies of the nozzle, 1J, 1S, and 1H were higher. Obviously, the use of plexiglass stage elements in impactors that sample charged particles is undesirable.

POLYDISPERSE AEROSOL SAMPLED WITH A BRINK IMPACTOR

Another set of experiments was done to investigate the possibility of charge effects at precipitator outlets. Figure 33 shows a schematic of the setup of the impactor and particle counter used in these experiments. Two stages of a Brink cascade impactor were employed with a removable polonium 210 α-source attached to the nozzle of the impactor. A flow rate of 2.83 ℓ/min (0.1 acfm) was maintained through the impactor using the pump in the Climet Particle Analyzer, an optical particle counter, which operates at 7.1 ℓ/min (0.25 acfm). Make-up air to the particle counter was supplied by a controlled, filtered, air supply. The aerosol exiting the impactor was charge neutralized with a second polonium 210 α-source to minimize sample and instrumental losses due to electrostatic forces between the impactor and particle counter.

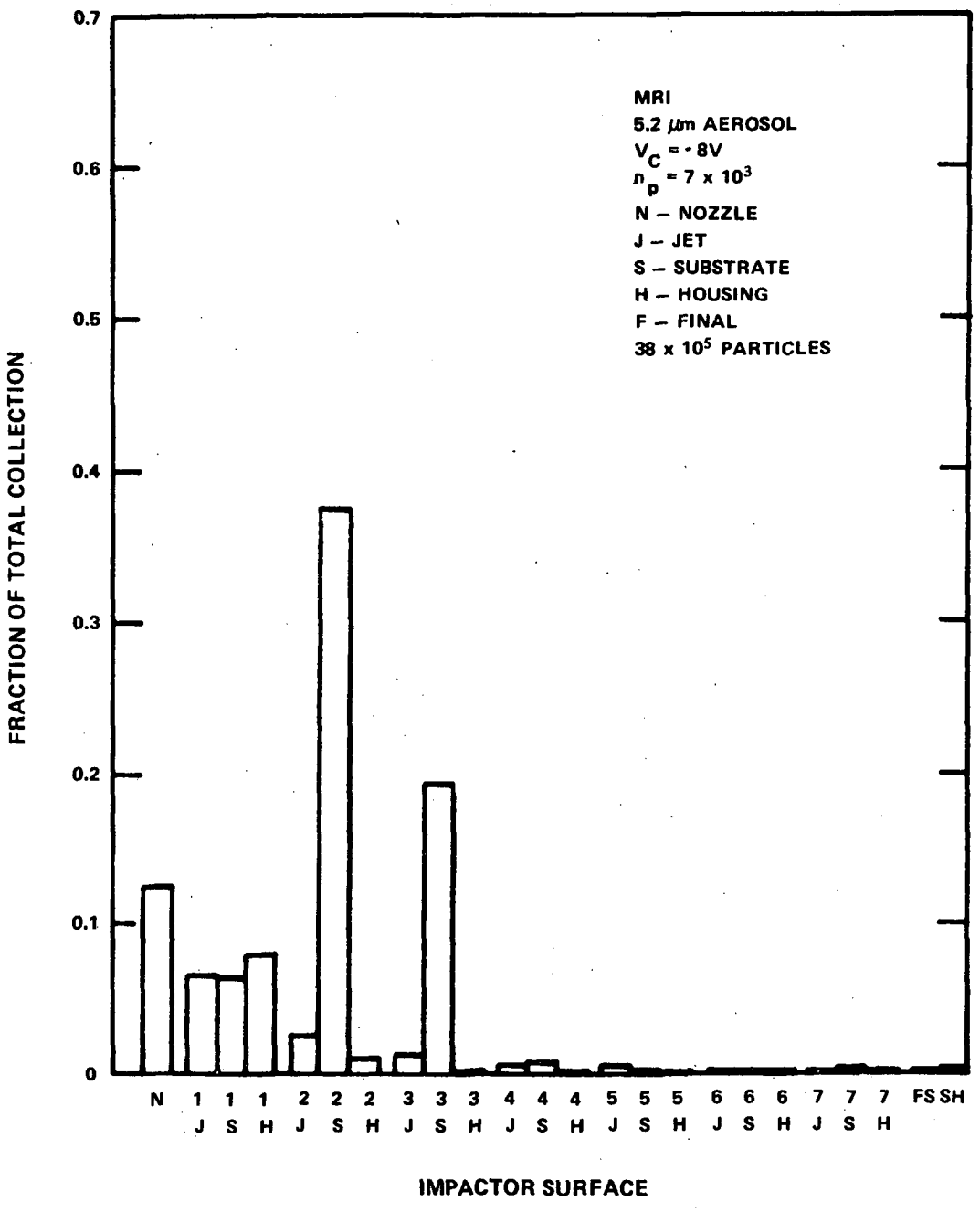

Figure 32. Sampling charged particles using MRI-Model 1502 Impactor with plexiglass jet plates, 2J, 3J, and 4J. (Other conditions are the same as the test depicted in Figure 11.)

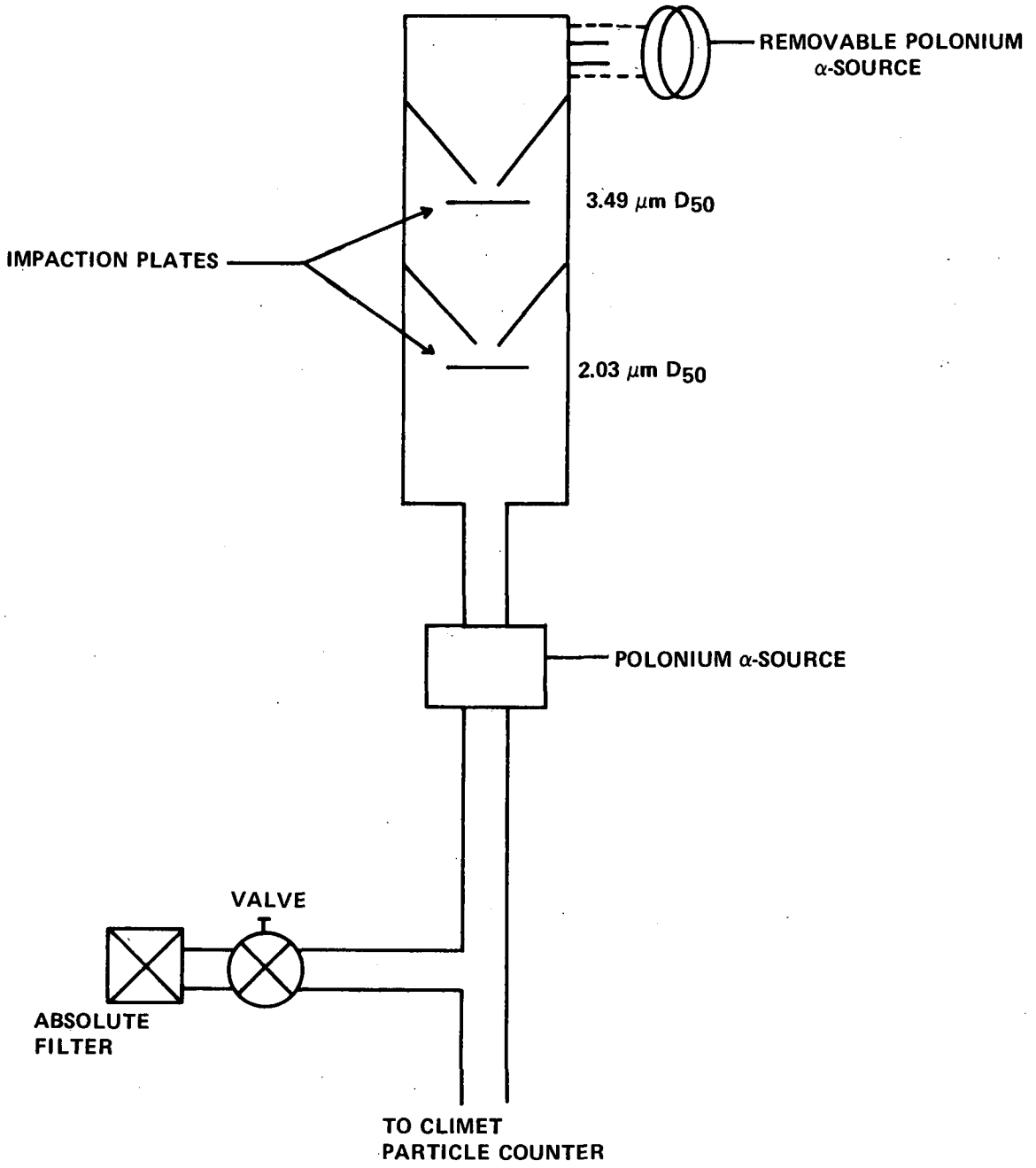

Figure 33. Sampling system used to sample charged polydisperse aerosols with a Brink cascade impactor.

The aerosol was produced by a "hobby" paint sprayer producing a polydisperse DOP aerosol which was sampled by the impactor at the outlet of a model wet-wall precipitator.

Four different configurations of the impactor were tested: (1) with glass-fiber filter substrates, (2) with bare metal plates, (3) with no plates (in order to study the effect of wall loss), and (4) extractive sampling with a 91 cm (3 ft), 6.35 mm (114 in) I.D. copper probe. Each condition was tested with and without the charge neutralizer attached to the impactor nozzle.

The data from this investigation are presented in Figures 34, 35, and 36. Figure 34 indicates that there is no appreciable effect of charge neutralization when glass-fiber filter substrates are used. Figure 35 indicates that there is some effect on the number of particles exiting the impactor with and without charge neutralization when bare metal plates are used. Figure 36 indicates that there may be substantial wall losses within the impactor which can be attributed to the electrostatic effects.

The results are plotted another way in Figure 37. The data are normalized to the concentration measured with the charge neutralizer in place. Curves are shown for the probe alone, for the impactor with glass-fiber substrates (no probe), and for the impactor operated with bare metal collection plates (no probe). Losses in the probe and with bare substrates are seen to be rather large. For the tests made using glass-fiber substrates there was no appreciable difference in the concentrations measured with and without the charge neutralizer.

The data from this study indicate that with a conducting substrate, such as bare metal, particle charge can indeed cause high increases in collection efficiency of an upper stage for small particles. However, with a nonconducting substrate little change was produced by particle charge.

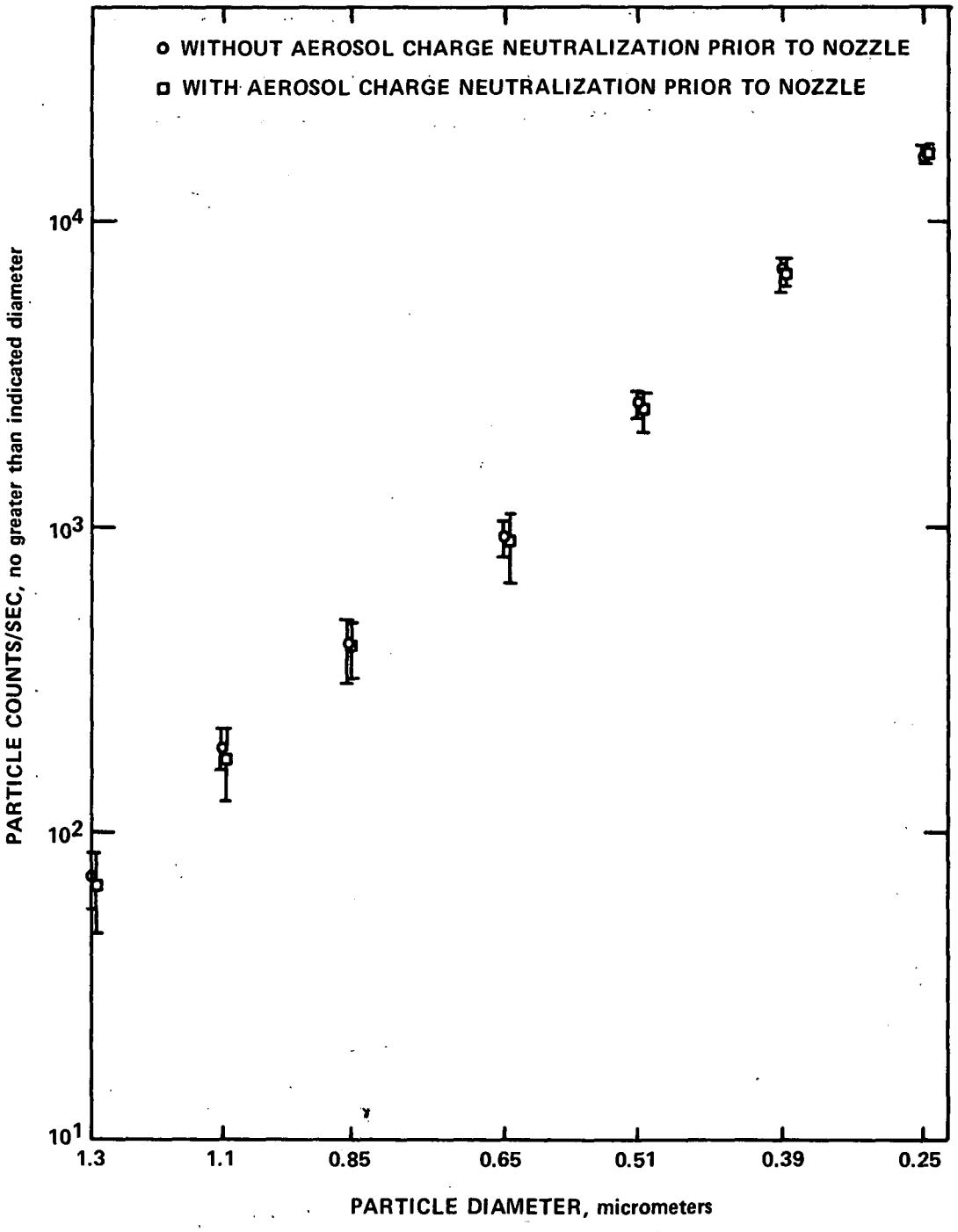

Figure 34. Particle concentration at the outlet of a Brink cascade impactor with glass-fiber filter substrates as collecting surfaces for charged and neutralized conditions. Error bars indicate one standard deviation.

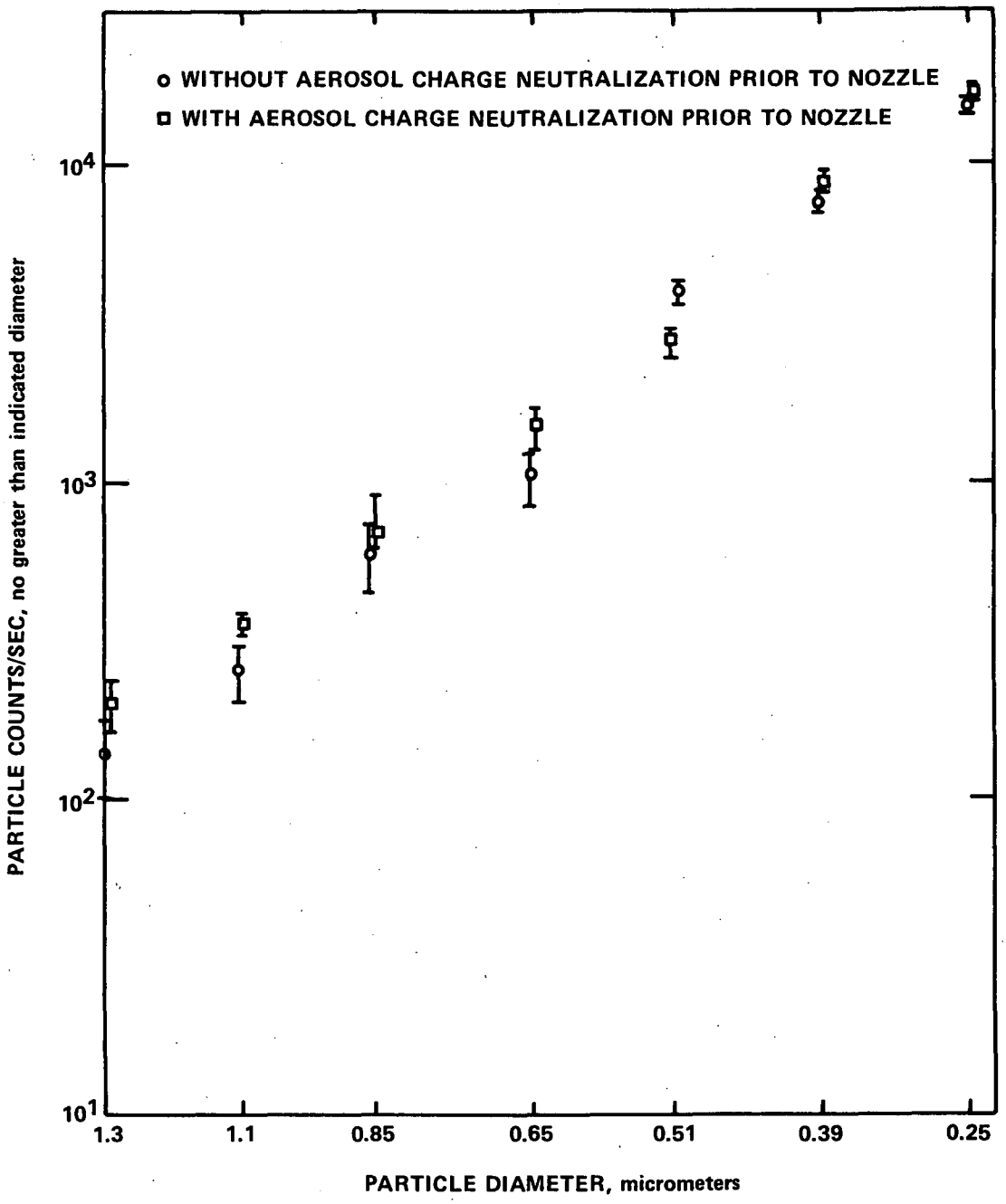

Figure 35. Particle concentration at the outlet of a Brink cascade impactor with bare metal plates as collection surfaces for charged and neutralized conditions. Error bars indicate one standard deviation.

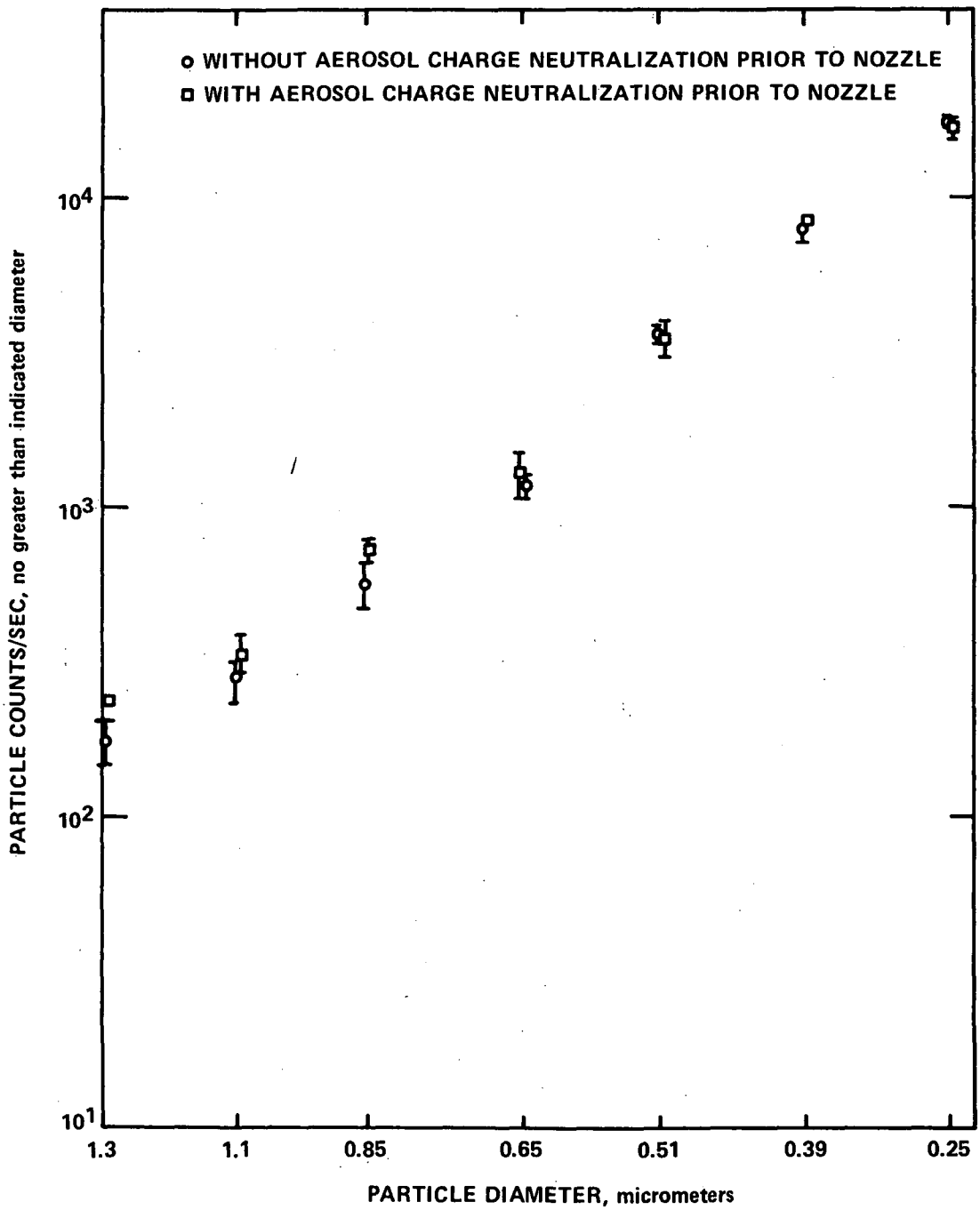

Figure 36. Particle concentration at the outlet of a Brink cascade impactor operated without particle collection surfaces (wall loss study) for charged and neutralized conditions. Error bars indicate one standard deviation.

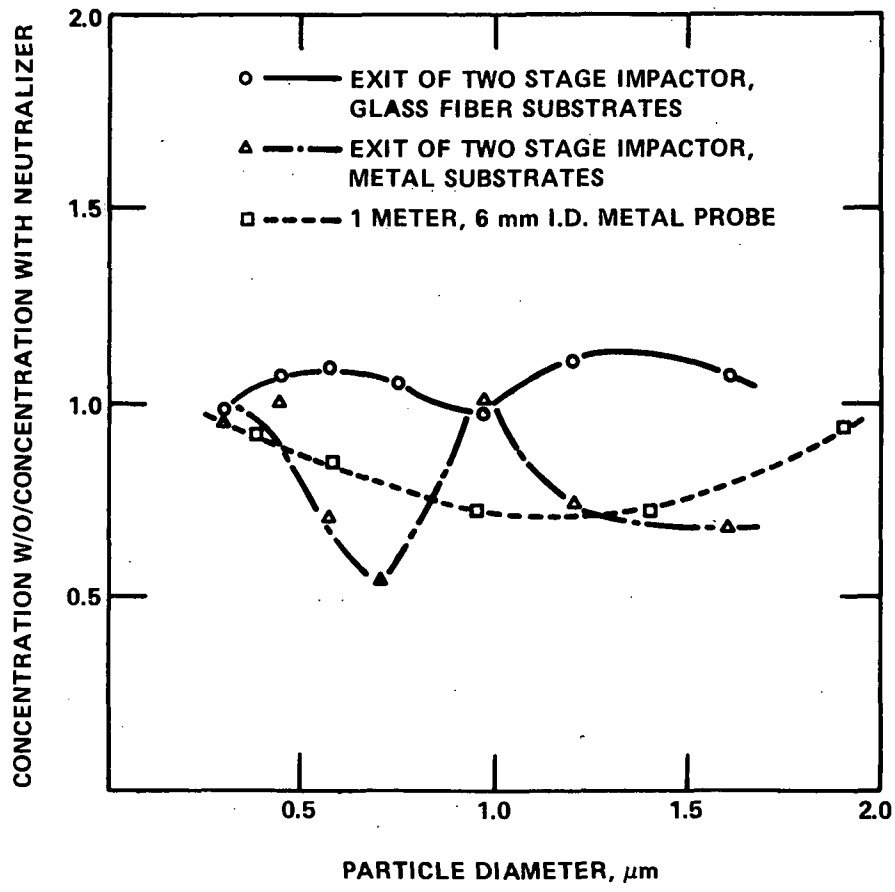

Figure 37. Particle losses in a Brink cascade impactor due to electrostatic forces.

POLYDISPERSE AEROSOL SAMPLED WITH AN ANDERSEN IMPACTOR

Another set of experiments was performed using two commercial cascade impactors to sample simultaneously a polydisperse ammonium fluorescein aerosol. One impactor sampled a charged aerosol while the other sampled a neutralized aerosol.

Experimental Apparatus

A schematic of the experimental apparatus is shown in Figure 38. A polydisperse aerosol of ammonium fluorescein was generated by an atomizer (RETEC X701N) and fed into a dispersion chamber. A compressed air line supplied dry, filtered air for dispersion, drying and atomization. Two pairs of opposed air jets perpendicular to the direction of the aerosol flow dispersed the air and initiated drying in the dispersion chamber. The aerosol flowed vertically through a 14 cm inner diameter (ID) plexiglass cylinder which functioned as a mixing and drying column, and two diffusional dryers. The diffusional dryers consisted of 90 mm ID, plexiglass cylinders with 30 mm ID, coaxial, cylindrical screens shown in Figure 38 by dotted lines. The screen cylinders were surrounded by 6-16 mesh silica gel desiccant. The particle charger as described by Bush and Smith[8] consisted of a disk-cylinder geometry. The disk electrode was 28.6 mm in diameter and 1.3 mm thick and was surrounded by an electrically grounded, 7.37 cm ID cylinder. Clear, plastic, 16-20 mm ID tubing connected the 25 mm ID, 90 mm long, plexiglass chambers to the charger. One chamber contained four polonium 210 strips (Staticmaster Model 3C500) bent into 25 mm-diameter circles while the other was empty. Each ion precipitator was 15 cm long and was constructed of a 9.5 mm outer diameter (OD) stainless steel tube electrically isolated and coaxial with a 17 mm ID stainless steel tube. The outer tube was electrically grounded and the inner tube was connected to a high voltage power supply. The ends of the inner tube were sealed with a bullet-shaped plug to minimize particle loss due to impaction and turbulence. Cascade impactors (Andersen Mark III Stack Sampler) with glass fiber substrates were connected to the

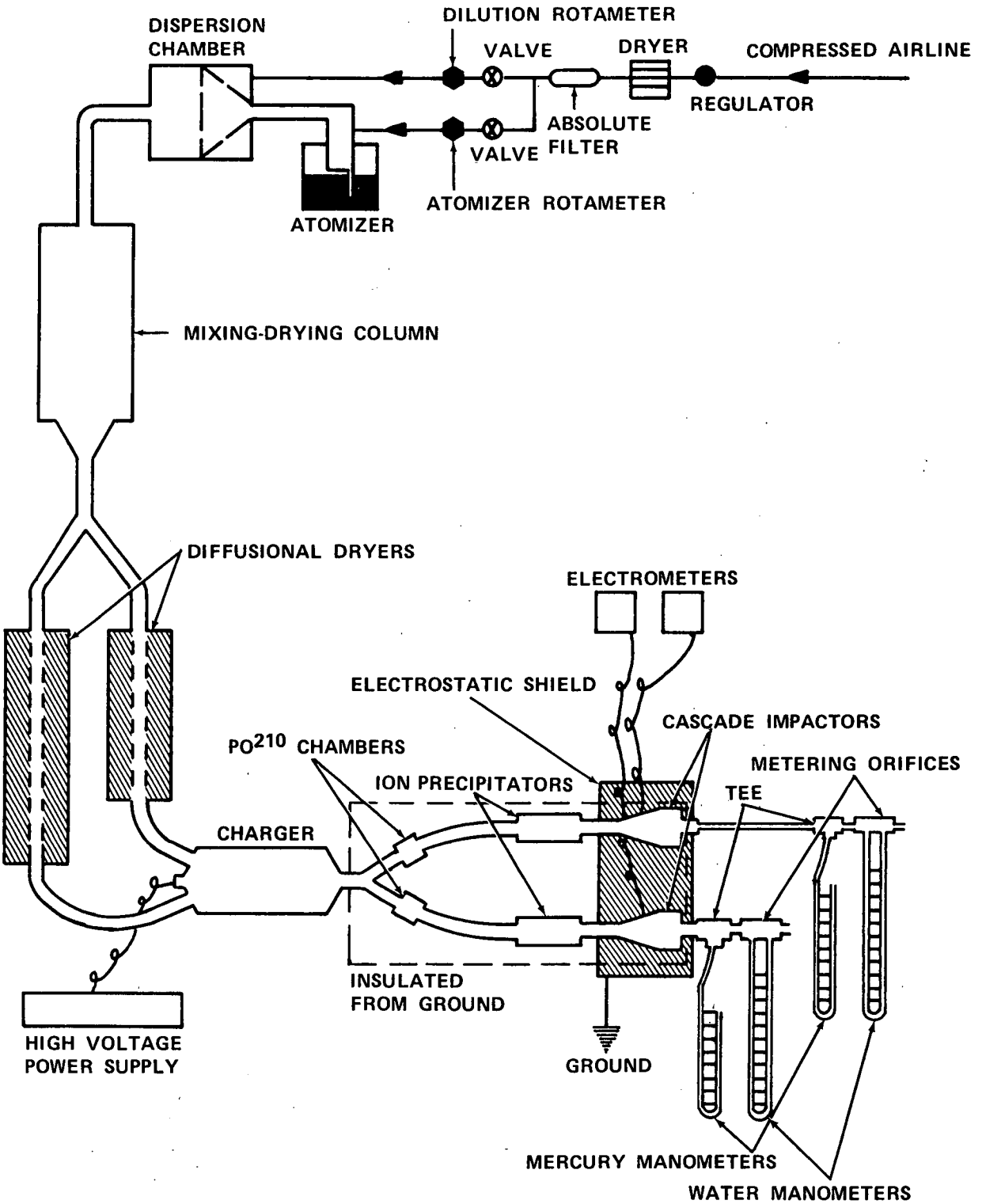

Figure 38. Polydisperse aerosol generating, charging, and sampling system.

ion precipitators with 9 mm ID, polyethylene tubing 23 mm long. Two calibrated metering orifices measured the flow exiting the impactors. The impactors were electrostatically shielded with a small mesh brass screen, and grounded through electrometers (Keithley No. 612C and No. 600B) measured the charge on the aerosol entering the impactors (through the Faraday cup principle).

Experimental Procedure

For each test, a polydisperse ammonium fluorescein aerosol was generated, dried, and passed through the system at a flowrate of 14.2 liters/min at the inlet of each impactor. Electrometers measured the charge collected on each impactor--a relatively low measurement for the neutralized aerosol branch as compared to the charged aerosol branch provided proof of sufficient neutralization. All tests were performed at ambient temperature with the pressure at the inlet to the impactors about 0.1 atm above ambient. After each test, the ammonium fluorescein particles collected on each impactor stage were dissolved in an ammonium hydroxide solution and analyzed in a spectrometer to determine the mass. Although no mass was noticed on the jet plates for most of the tests, each plate was rinsed and grouped with the substrate below it for the mass determination. The data from each impactor test was reduced using the procedures described by McCain, et al.[9] This data is presented in the form of computer plots of the differential mass concentration vs. particle diameter in Figures 39-44. Figures 39 and 40 show actual mass concentrations in mg/m^3 and Figures 41-44 list average, normalized mass concentrations in arbitrary units. Errors bars indicate 90 percent confidence limits.

System Equivalency

Initially, tests were performed to ascertain that the mass concentrations and the particle size distributions entering both impactors were identical. In these tests both impactors sampled

the same aerosol from alternate branches. In the first four tests the charger was not operating and the impactors sampled the uncharged aerosol. In the next three tests, the charger was operated and the aerosol sampled was charged in an electric field of 6.9×10^5 V/m Impactors sampled alternately from each branch to determine if there were any differences in the performances of the impactors.

Charged and Neutralized Particle Sampling

These tests were similar to the charged aerosol tests described above, but with four polonium 210 sources in one branch of the system. It was experimentally determined that four sources were sufficient to neutralize the charged particles exiting the charger.

Although the effectiveness of the charge neutralizers was demonstrated, attempts to measure the charge level of the charged, aerosol fraction accurately were unsuccessful. The current level was very low and stray currents in the charge collection/measurement systems resulted in a low signal-to-noise ratio. The ion precipitators were used to remove ion charges produced by the polonium 210 that might influence the particulate charge measurements. Electric fields of 13 and 2.7 kV/m were used and produced identical results. Particulate loss in the branch upstream of an impactor was concentrated in the ion precipitators and amounted to no more than 5 percent of the total mass of the particles entering the branch, being greater for the charged particles.

The tests in which charged and neutralized aerosols were sampled simultaneously can be divided into four conditions. These conditions are identified by the strength of the electric field within which the particles were charged and by the mass median diameter of the aerosol as given in Table III.

Table III. Summary of Polydisperse Aerosol Test Conditions

Condition	A	B	C	D
Tests	2-5	7-8	9-12	15-18
Mass Median Diameter, μm	1.27	1.02	.692	1.01
Electric Field x 10^6 V/m	6.1	6.1	6.3	8.3

An approximate calculation of the total charge accumulated by an aerosol particle of radius r in an electric field E is given by Pontius et al.[10] to be.

$$n_p = \pi r C_1 \left\{ \frac{\mu r E N t}{\mu N t + C_1} \left[1+2\left(\frac{k-1}{k+2}\right)\right] + C_2 T \ln\left(\frac{rvNt}{C_1 C_2 T} + 1\right)\right\}$$

where

$$C_1 = \frac{4\varepsilon_0}{e}, \quad C_2 = \frac{K}{e}$$

and

t = particle residence time (sec),
k = particle dielectric constant,
e = electron charge (coul),
ε_0 = permittivity of free space (fd/m),
μ = ion mobility ($m^2/V \cdot sec$),
T = temperature (°K)
K = Boltzmann's constant (j/°K), and
v = mean thermal ion speed (m/sec).

This calculation for five particle sizes indicates the relative difference between "moderate" and "high" charge levels, and is given for each test condition in Table IV. The data is presented as a ratio of the charge calculated for the conditions of each test divided by the charge calculated for conditions representative of those found at industrial electrostatic precipitators. Conditions A, B, and C are considered moderate charge conditions and condition D is considered a high charge condition.

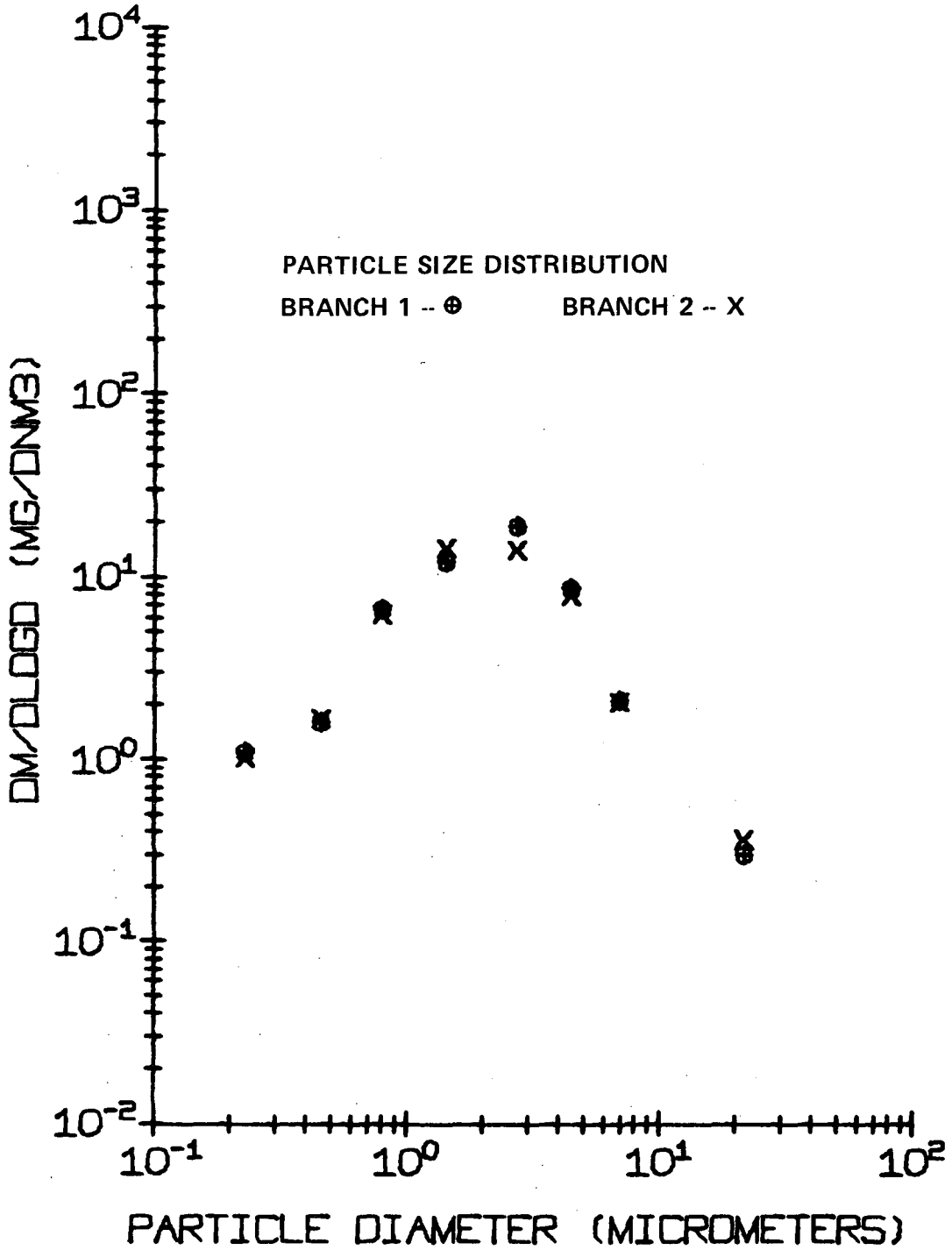

Figure 39. Particle size distribution ----- dM/dLog D versus particle diameter. Both impactors sampling an uncharged aerosol simultaneously.

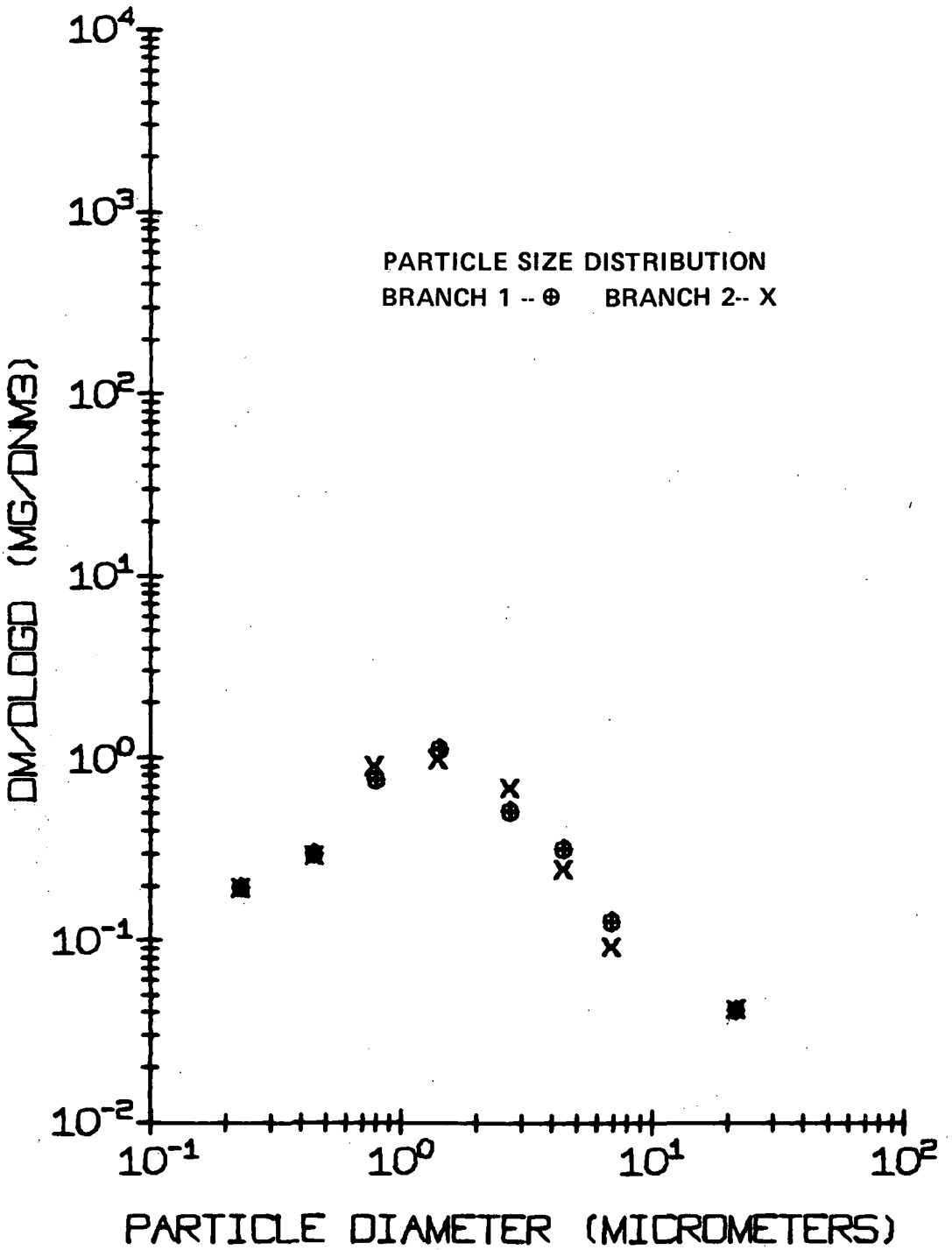

Figure 40. Particle size distribution ----- d M/dLog D versus particle diameter. Both impactors sampling a charged aerosol simultaneously.

Table IV. Calculated Charge on Charged Aerosol Particles Relative to that Expected in a Full Scale Precipitator

Diameter, μm / Condition	0.1	0.5	1.0	2.0	5.0
A	1.1	1.3	1.4	1.4	1.5
B	1.0	1.3	1.3	1.4	1.5
C	1.1	1.3	1.4	1.5	1.5
D	1.4	1.7	1.8	1.9	2.0

Results

The results of the system equivalency tests are summarized in Table V and illustrations of typical results are shown in Figures 39 and 40. The aerosol concentrations as measured by the cascade impactors for the tests conducted at both conditions are given in Table V. The mass concentrations for the charged condition were lower due to the loss of particles in the charger. The figures show that the particle size distributions in both branches were identical. Evidence that the two impactors performed identically was demonstrated by the fact that the impactors sampled alternating branches for each consecutive test without causing an appreciable difference in the size distribution plots.

Table V. System Branch Equivalency Data

Date	Test	Condition	Aerosol Concentration (mg/m^3) Branch 1	Branch 2
10/3/77	1	Uncharged	15.2	16.0
10/4	1	Uncharged	13.8	13.1
10/5	1	Uncharged	14.4	13.6
10/6	1	Uncharged	14.2	13.7
10/6	2	Charged	0.91	0.88
10/7	1	Charged	0.97	0.79
10/7	2	Charged	0.96	0.97

Figures 41 through 44 show the results of the charged and neutralized particulate sampling.

The ratio of the average calculated charge of the laboratory aerosol to the typical charge on an aerosol exiting the outlet of an industrial electrostatic precipitator is given for five particle sizes in the legend of each figure. In each case, more mass was caught on the upper stages of the impactor sampling the charged aerosol than in the one sampling the neutralized aerosol. This effect is most noticeable for particle sizes larger than 2.9 μm for conditions A, B, and D, and sizes larger than 1.0 μm for condition C. The larger differences occur for condition D where the particles have a higher charge than those in the other conditions. For all four conditions, approximately the same amount of mass is collected on the stages with D_{50}'s close to the mass median diameter of the aerosol for both neutral and charged impactors. For all conditions, relatively more mass was collected on the lower stages of the impactor sampling the neutralized aerosol than on the impactor sampling the charged aerosol. For moderate particle charge, this mass difference is very slight. For the higher particle charge, the mass difference becomes noticeable (Figure 44).

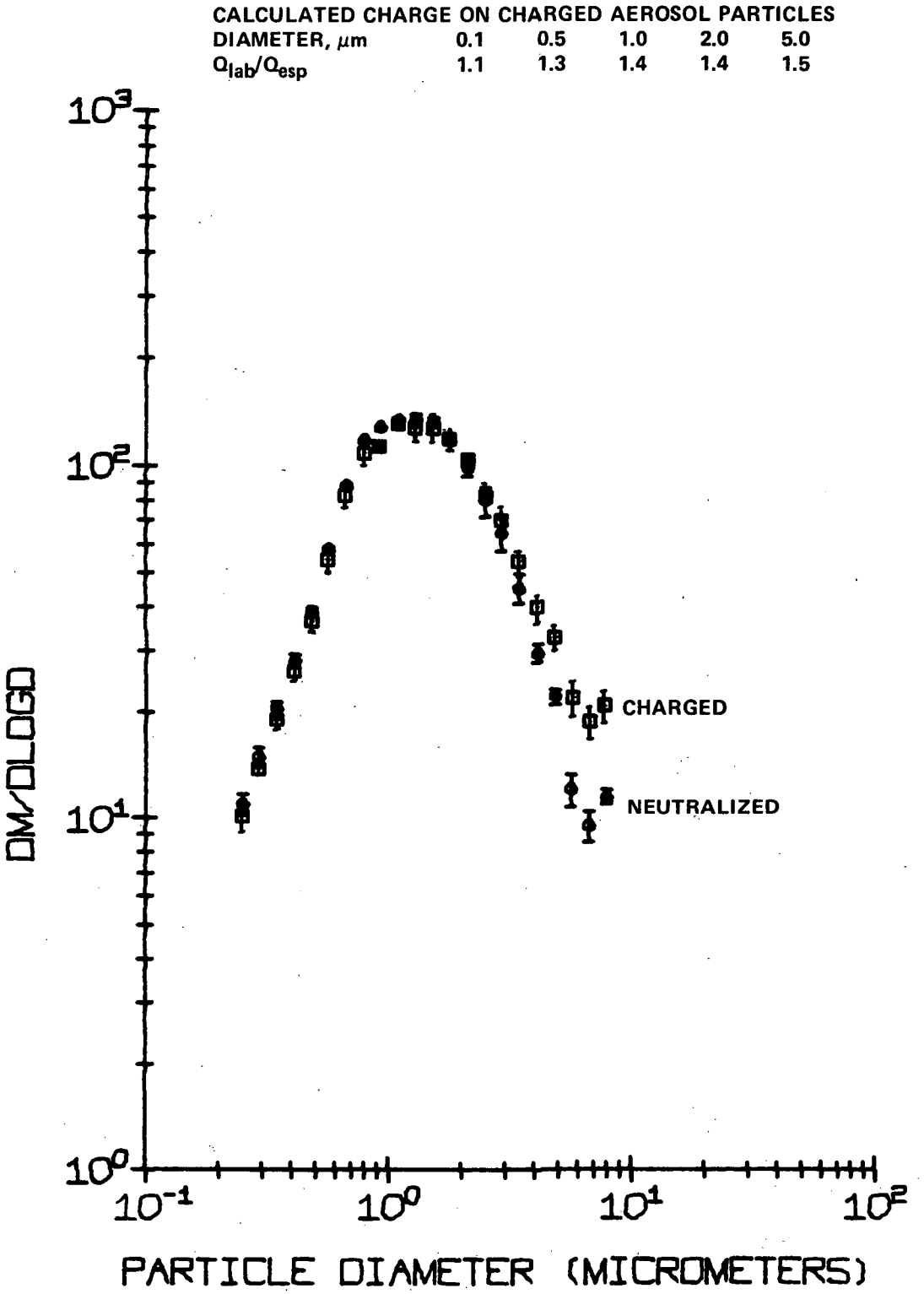

Figure 41. Particle size distribution for moderate charging condition for a mass median diameter of 1.27 micrometers.

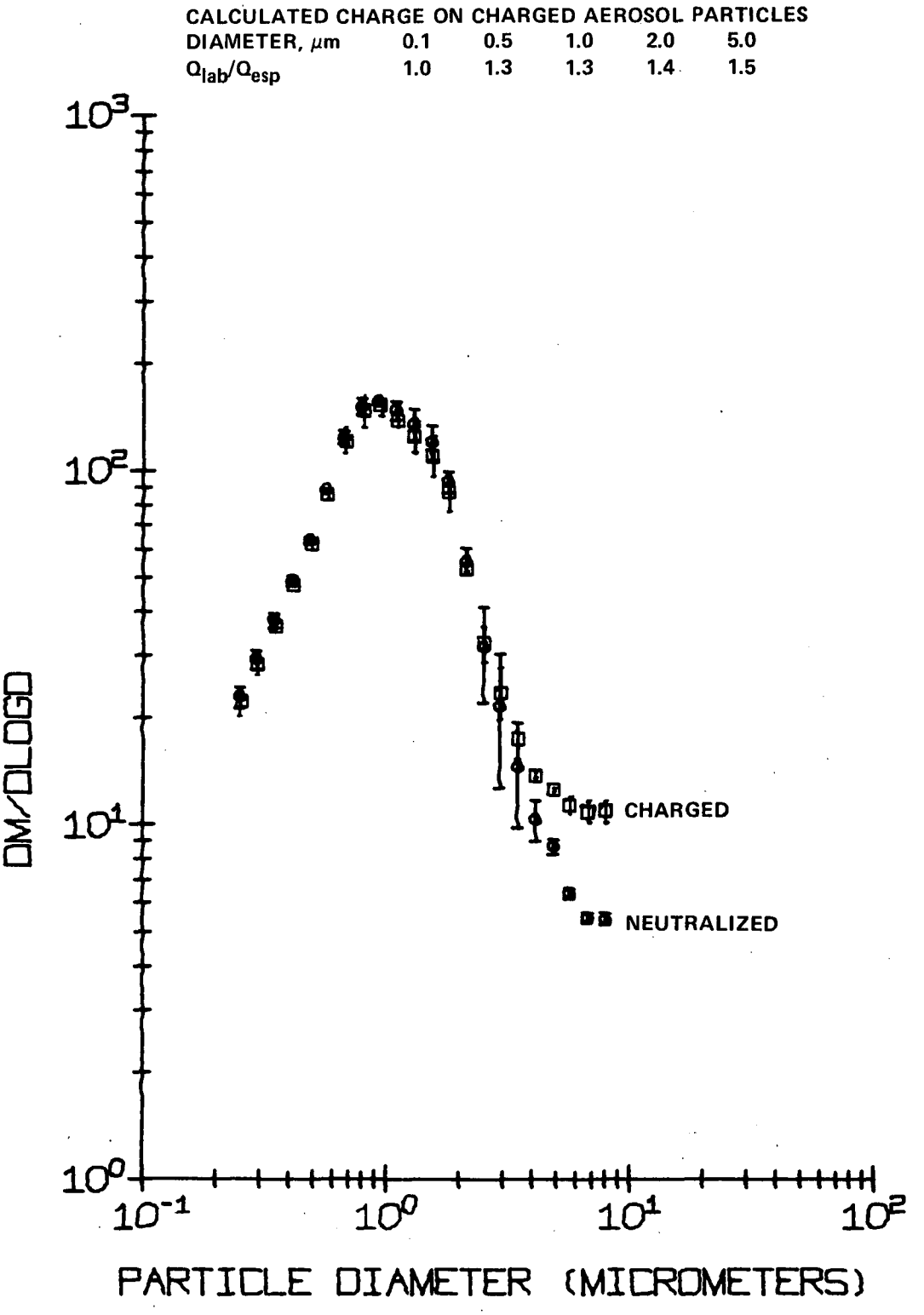

Figure 42. Particle size distribution for moderate charging condition for a mass median diameter of 1.02 micrometers.

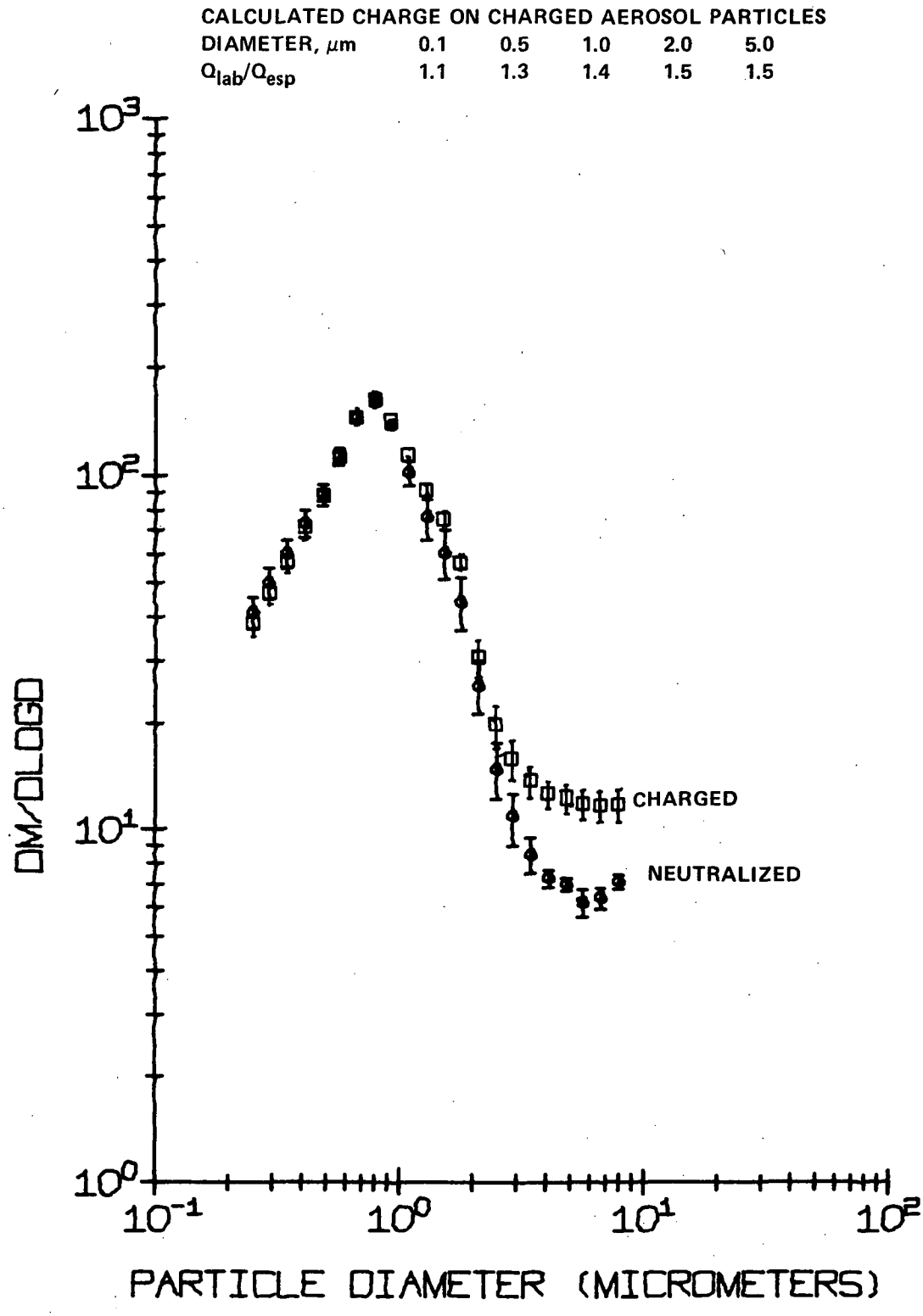

Figure 43. Particle size distribution for moderate charging conditions for a mass median diameter of 0.692 micrometer.

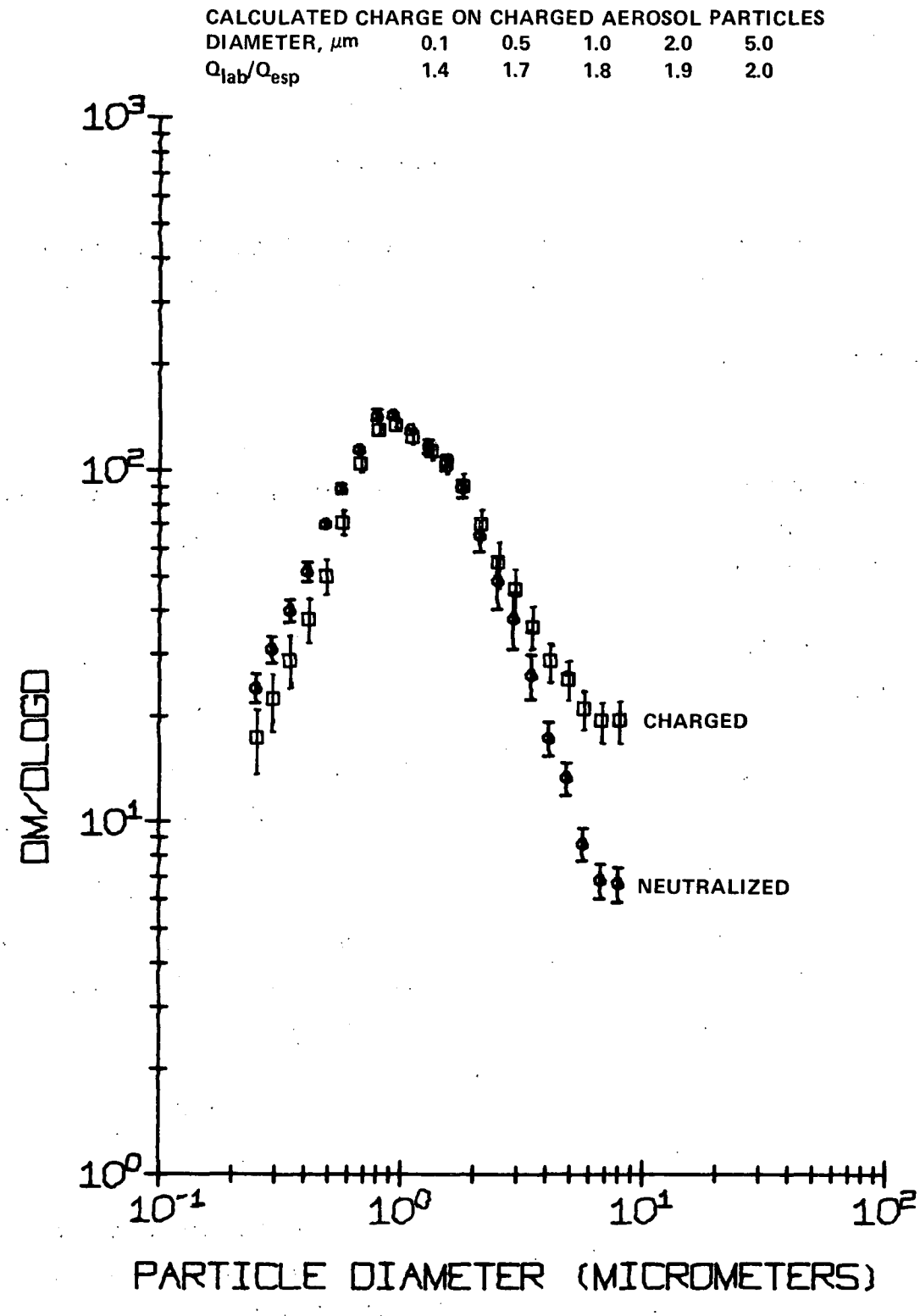

Figure 44. Particle size distribution for high charging conditions for a mass median diameter of 1.01 micrometers.

SECTION 3.

SUMMARY AND CONCLUSIONS

A review of the important parameters and conclusions for each experiment are contained in the following lists:

MONODISPERSE AEROSOL

1. Tests were done with the impactors operated at the recommended flow rate and with particle charges equivalent to those expected at precipitator outlets. However, only two particle sizes were used.

2. Wall losses were measured along with the stage collection efficiency.

3. For charge levels approximately five times higher than those expected at a precipitator outlet, very large effects were noted.

4. For samples taken using glass-fiber substrates at representative particle charge levels, the effect of particle charge on impactor performance was found to be minimal.

5. Grounding the impactors generally increased stage collection efficiencies.

6. The general effect of charge was to reduce the sharpness (slope) of the curve at values of $\sqrt{\psi}$ below the peak while not charging $\sqrt{\psi_{50}}$ (or the stage D_{50}) significantly. At large values of $\sqrt{\psi}$, the effect of particle charge was to reduce the efficiency in a manner similar to particle bounce.

7. The data from this experiment were not taken with particle concentrations high enough to be representative of those to be found at the outlet of industrial precipitators.

POLYDISPERSE AEROSOL SAMPLED WITH A BRINK IMPACTOR

1. Tests were done with the impactors operated at the recommended flow rate with a polydisperse aerosol and particle charges equivalent to those expected at precipitator outlets. Only two stages of a Brink impactor were used.

2. The particle concentration was less than would be expected at a precipitator outlet.

3. A test on wall losses showed that they play a significant part in impactor performance when a charged aerosol is sampled.

4. Tests using glass-fiber substrate did not show an appreciable difference in the collection of charged and uncharged particles. Tests using bare metal substrates, however, showed quite a difference between the collection of charged particles and the collection of uncharged particles.

POLYDISPERSE AEROSOL SAMPLED WITH ANDERSEN IMPACTORS

1. Tests were performed with entire Andersen impactors operated at the recommended flow rate and with glass-fiber substrates only.

2. The particle concentration was similar to that expected at the outlet of an industrial electrostatic precipitator. The aerosol contained polydisperse ammonium fluorescein particles.

3. Wall losses were not considered separately, however, no visible wall loss was observed for tests with particles having moderate charge (typical of ESP outlets). The wall losses were visibly evident in the high charge tests.

4. Moderate particle charge levels had little effect on impactor performance for the middle and lower stages. For stages with D_{50}'s above 3 micrometers, up to about twice as much mass was caught in the charged particle impactor than in the neutral one.

5. For charging conditons higher than those considered moderate here, the effects of particle charge were more significant both for the lower impactor stages and the upper impactor stages, with the middle stages giving approximately true mass measurements.

REFERENCES

1. Cushing, K. M., G. E. Lacey, J. D. McCain, and W. B. Smith. Particle Sizing Techniques for Control Device Evaluation: Cascade Impactor Calibration. EPA-600/2-76-280, U.S. Environmental Protection Agency, Research Triangle Park, N.C., 1976. 79 pages.

2. Reischl, G., W. John, and W. Devor. Uniform Electrical Charging of Monodisperse Aerosols. J. Aerosol Sci., 8:55-65, 1977.

3. Sem, G. J. Submicron Particle Size Measurement of Stack Emissions Using the Electrical Mobility Technique. In: Proceedings of the Workshop on Sampling, Analysis, and Monitoring of Stack Emissions, Electric Power Research Institute, Dallas, Texas, 1975. pp. 111-129.

4. Zung, J. T., and C. C. Snead. Evaporation Kinetics of Liquid Droplets. U.S. Dept. of Army, Edgewood Arsenal-DAAA-15-67-C-0151, Field Evaluation Division, Edgewood Arsenal, Maryland 21010, 1968. 116 pages.

5. Cooper, D. W., and J. W. Davis. Cascade Impactors for Aerosols: Improved Data Analysis. Amer. Ind. Hyg. Assoc., p. 79, 1972.

6. Cooper, D. W., and L. A. Spielman. Data Inversion Using Nonlinear Programming with Physical Constraints: Aerosol Size Distribution Measurement by Impactors. Atmos. Environ., 10, pp. 723-729, 1976.

7. Picknett, R. G. A New Method of Determining Aerosol Size Distributions from Ministage Sampler Data. Aerosol Sci., 1972.

8. Bush, P. V., and W. B. Smith. An Electrostatic Precipitator Backup for Sampling Systems. EPA-600/7-78-114, U.S. Environmental Protection Agency, Research Triangle Park, N.C., 1978. 35 pp.

9. Johnson, J. W., G. I. Clinard, L. G. Felix, and J. D. McCain. A Computer-Based Cascade Impactor Data Reduction System. EPA-600/7-78-042, U.S. Environmental Protection Agency, Research Triangle Park, N.C., 1978. 601 pp.

10. Pontius, D. H., L. G. Felix, J. R. McDonald, and W. B. Smith. Fine Particle Charging Development. EPA-600/2-77-173, U.S. Environmental Protection Agency, Research Triangle Park, N.C., 1977. 240 pp.

TECHNICAL REPORT DATA
(Please read Instructions on the reverse before completing)

1. REPORT NO.	2.	3. RECIPIENT'S ACCESSION NO.
EPA-600/7-79-027		

4. TITLE AND SUBTITLE	5. REPORT DATE
Sampling Charged Particles with Cascade Impactors	January 1979
	6. PERFORMING ORGANIZATION CODE

7. AUTHOR(S)	8. PERFORMING ORGANIZATION REPORT NO.
W. E. Farthing, D. H. Hussey, W. B. Smith, and R. R. Wilson, Jr.	SORI-EAS-79-024

9. PERFORMING ORGANIZATION NAME AND ADDRESS	10. PROGRAM ELEMENT NO.
Southern Research Institute 2000 Ninth Avenue, South Birmingham, Alabama 35205	EHE624
	11. CONTRACT/GRANT NO.
	68-02-2131, T.D. 10401 and 11301

12. SPONSORING AGENCY NAME AND ADDRESS	13. TYPE OF REPORT AND PERIOD COVERED
EPA, Office of Research and Development Industrial Environmental Research Laboratory Research Triangle Park, NC 27711	Task Final; 4/77 - 9/78
	14. SPONSORING AGENCY CODE
	EPA/600/13

15. SUPPLEMENTARY NOTES IERL-RTP project officer is D. Bruce Harris, Mail Drop 62, 919/541-2557.

16. ABSTRACT The report discusses three sets of experiments which demonstrate that a cascade impactor sampling a charged aerosol may yield a particle size distribution measurement that deviates from the time distribution. The distributions indicated more large particles and fewer small particles than actually existed, due to the particles' attraction to the grounded impactor plates (stages). Although higher charge levels produced larger deviations from the true size distribution, the magnitude of the deviation and the corresponding correction factor for any given charged aerosol are unpredictable. Also, the error was smaller if glass fiber substrates were used as collection surfaces instead of bare metal. For electrostatic precipitators operating at normal charging conditions (an electric field of 400,000 V/m and a current density of 0.0003 A/sq m/s), the size distribution (measured by the lower stages of an Andersen cascade impactor with glass fiber substrates) was not significantly different from the true size distribution.

17. KEY WORDS AND DOCUMENT ANALYSIS

a. DESCRIPTORS		b. IDENTIFIERS/OPEN ENDED TERMS	c. COSATI Field/Group	
Pollution	Dust	Pollution Control	13B	11G
Sampling	Size Determination	Stationary Sources	14B	
Measurement	Electrostatic Precipitators	Cascade Impactors		
Impactors		Andersen Impactors	13I	
Charged Particles	Glass Fibers	Time Distribution	20H	11B
Aerosols	Substrates		07D	11D

18. DISTRIBUTION STATEMENT	19. SECURITY CLASS *(This Report)*	21. NO. OF PAGES
Unlimited	Unclassified	88
	20. SECURITY CLASS *(This page)*	22. PRICE
	Unclassified	

EPA Form 2220-1 (9-73)